Journal Pre-proof

A comparative analysis of the partitioning behaviour of SARS-CoV-2 RNA in liquid and solid fractions of wastewater

Patrick R. Breadner, Hadi A. Dhiyebi, Azar Fattahi, Nivetha Srikanthan, Samina Hayat, Marc G. Aucoin, Scott J. Boegel, Leslie M. Bragg, Paul M. Craig, Yuwei Xie, John P. Giesy, Mark R. Servos

Please cite this article as: P.R. Breadner, H.A. Dhiyebi, A. Fattahi, et al., A comparative analysis of the partitioning behaviour of SARS-CoV-2 RNA in liquid and solid fractions of wastewater, *Science of the Total Environment* (2023), https://doi.org/10.1016/j.scitotenv.2023.165095

This is a PDF file of an article that has undergone enhancements after acceptance, such as the addition of a cover page and metadata, and formatting for readability, but it is not yet the definitive version of record. This version will undergo additional copyediting, typesetting and review before it is published in its final form, but we are providing this version to give early visibility of the article. Please note that, during the production process, errors may be discovered which could affect the content, and all legal disclaimers that apply to the journal pertain.

A comparative analysis of the partitioning behaviour of SARS-CoV-2 RNA in liquid and solid fractions of wastewater

Patrick R. Breadner[a], Hadi A. Dhiyebi[a], Azar Fattahi[a], Nivetha Srikanthan[a], Samina Hayat[a], Marc G. Aucoin[b], Scott J. Boegel[b], Leslie M. Bragg[a], Paul M. Craig[a], Yuwei Xie[c,d], John P. Giesy[d,e] and Mark R. Servos[a]

[a] Department of Biology, University of Waterloo, 200 University Ave W, Waterloo, Ontario, Canada, N2L 3G1
[b] Department of Chemical Engineering, University of Waterloo, 200 University Ave W, Waterloo, Ontario, Canada, N2L 3G1
[c] Key Laboratory of Pesticide Environmental Assessment and Pollution Control, Nanjing Institute of Environmental Sciences, Ministry of Ecology and Environment, Nanjing, China, 210042
[d] Toxicology Centre, University of Saskatchewan, 44 Campus Dr, Saskatoon, Saskatchewan, Canada, S7N 5B3
[e] Department of Environmental Science, Baylor University, One Bear Place, Waco, Texas, USA, 76798

Corresponding Author:
Mark R. Servos
mservos@uwaterloo.ca

1

Abstract

As fragments of SARS-CoV-2 RNA can be quantified and measured temporally in wastewater, surveillance of concentrations of SARS-CoV-2 in wastewater has become a vital resource for tracking the spread of COVID-19 in and among communities. However, the absence of standardized methods has affected the interpretation of data for public health efforts. In particular, analyzing either the liquid or solid fraction has implications for the interpretation of how viral RNA is quantified. Characterizing how SARS-CoV-2 or its RNA fragments partition in wastewater is a central part of understanding fate and behaviour in wastewater. In this study, partitioning of SARS-CoV-2 was investigated by use of centrifugation with varied durations of spin and centrifugal force, polyethylene glycol (PEG) precipitation followed by centrifugation, and ultrafiltration of wastewater. Partitioning of the endogenous pepper mild mottled virus (PMMoV), used to normalize the SARS-CoV-2 signal for fecal load in trend analysis, was also examined. Additionally, two surrogates for coronavirus, human coronavirus 229E and murine hepatitis virus, were analyzed as process controls. Even though SARS-CoV-2 has an affinity for solids, the total RNA copies of SARS-CoV-2 per wastewater sample, after centrifugation (12,000 g, 1.5 h, no brake), were partitioned evenly between the liquid and solid fractions. Centrifugation at greater speeds for longer durations resulted in a shift in partitioning for all viruses toward the solid fraction except for PMMoV, which remained mostly in the liquid fraction. The surrogates more closely reflected the partitioning of SARS-CoV-2 under high centrifugation speed and duration while PMMoV did not. Interestingly, ultrafiltration devices were inconsistent in estimating RNA copies in wastewater, which can influence the interpretation of partitioning. Developing a better understanding of the fate of SARS-CoV-2 in wastewater and creating a foundation of best practices is the key to supporting the current pandemic response and preparing for future potential infectious diseases.

1. Introduction

Wastewater-based surveillance (WBS) has emerged as an important tool in supporting Public Health Units (PHUs) during the COVID-19 pandemic (Hrudey et al., 2022). As people contract COVID-19, they shed fragments of RNA of the SARS-CoV-2 virus in their feces as well as other bodily fluids that can enter municipal wastewater sewer systems. These fragments of RNA can then be quantified over time to track status and trends as well as infer the relative numbers of persons infected with COVID-19 in a community (Manuel et al., 2022; Medema et al., 2020; Wurtzer et al., 2020). A key advantage of WBS is its broad-stroke approach to community-level surveillance, its inclusion of both symptomatic and asymptomatic individuals, and independence of clinical testing. It is not affected by socioeconomic factors that can influence access to clinical testing and bias results for various sub-populations (Safford et al., 2022; WHO, 2022). Furthermore, it can be adapted to congregate settings, such as long-term care homes, prisons, and schools as well as northern, remote, and isolated communities (Hrudey et al., 2022; Manuel et al., 2022; Respiratory Virus Infections Working Group, 2020). In Ontario, Canada, WBS has become especially important for PHUs since clinical testing eligibility was restricted at the end of 2021, which was coincident with emergence of the Omicron variant of SARS-CoV-2.

Despite the expansion of WBS during the COVID-19 pandemic, there has not yet been a standardization of methods used to measure RNA of SARS-CoV-2 in wastewater. Many approaches, of variable effectiveness, have been used for isolation and concentration of RNA of SARS-CoV-2 from wastewater. Some of these methods include direct capture of the solids following centrifugation or ultracentrifugation, ultrafiltration, electronegative membrane adsorption, and PEG precipitation (La Rosa et al., 2020). In principle, all of these methods are designed to achieve the same goal, which is to isolate and concentrate viral RNA from a wastewater sample. However, because they are fundamentally different in their approaches, they do not necessarily provide equivalent estimates of amounts of SARS-CoV-2 RNA in wastewater (Chik et al., 2021; Pecson et al., 2021). Methods based on ultrafiltration usually concentrate virus using a membrane of a selected pore size, which is usually after centrifugation or

filtration, to remove the larger particles that would tend to occlude the pores and limit the effectiveness of accurate ultrafiltration of RNA. Methods based on centrifugal force are sometimes combined with chemicals, such as polyethylene glycol (PEG) and NaCl, to facilitate aggregation/precipitations of viral RNA to form a pellet. While some practitioners use whole influent, typically, selected methods ignore the virus that exists in one of the phases.

The partitioning behaviour of viruses in wastewater is not well understood. Methods for concentrating SARS-CoV-2 from wastewater have targeted the solid fraction (e.g., pelleted solids post centrifugation), the liquid fraction (e.g., concentrate from ultrafiltration), or both the liquid and solid fraction together (e.g., PEG precipitation with or without centrifugation) (Chik et al., 2021; Pecson et al., 2021). Both liquid-based (Medema et al., 2020; Wu et al., 2020) and solid-based (D'Aoust et al., 2021; Kitamura et al., 2021) methods have been useful for quantifying SARS-CoV-2 RNA in wastewater. However, recently, there has been a strong emphasis for methods based on solids (Chik et al., 2021; D'Aoust et al., 2021; Graham et al., 2021; Kim et al., 2022; Kitamura et al., 2021). While it is clear that SARS-CoV-2 or its RNA is associated with the solids fraction (Kim et al., 2022), the fact that ultrafiltration methods can also be used to quantitate and track trends of the SARS-CoV-2 signal suggests that a large portion remains in the liquid fraction. With that said, the survivability of SARS-CoV-2 and its RNA in different water matrices might be affected by the presence of organic matter, which can cause the viruses to be encapsulated within or adsorb onto the organic particles (Gundy et al., 2008; Paul et al., 2021; Wellings et al., 1976). In turn, this might also make the viral material less vulnerable to disinfectants and other antiviral agents (Paul et al., 2021). The viral material that is associated with the organic matter can be targeted by settling out these particles (Gundy et al., 2008). The apparent partitioning of the SARS-CoV-2 virus or its RNA is likely affected by the presence and characteristics of organic matter in wastewater and the methods applied, which may affect interpretations of surveillance data.

Due to limitations of working directly with SARS-CoV-2, a surrogate can be used that has a similar partitioning behaviour to the target virus in wastewater and estimate recovery and monitor the

4

performance of the method. Human coronavirus 229E (229E) and murine hepatitis virus (MHV), which are closely related to SARS-CoV-2 in the Coronaviridae family (International Committee on Taxonomy of Viruses, 2021), have been used as surrogates for SARS-CoV-2 (Ahmed et al., 2020; Graham et al., 2021; Islam et al., 2022; Mondal et al., 2021). Due to their morphological similarities, including presence of an enveloped membrane, positive-strand RNA, and spherical shape with spike proteins (Artika et al., 2020), these viruses are expected to behave similarly in wastewater. The pepper mild mottled virus (PMMoV) is an enteric virus that is ubiquitous in wastewater (Kitajima et al., 2018) that has been commonly used to normalize SARS-CoV-2 surveillance data for fecal load in wastewater (Aguiar-Oliveira et al., 2020; Chik et al., 2021; D'Aoust et al., 2021; Wu et al., 2020). In some cases, normalizing against PMMoV has improved the SARS-CoV-2 trends over time (D'Aoust et al., 2021) but in most cases, it did not improve or even worsen correlations between the SARS-CoV-2 signal and clinical cases of COVD-19 (Ai et al., 2021; Dhiyebi et al., 2023b; Feng et al., 2021). Thus, understanding the partitioning behaviour of PMMoV compared to SARS-CoV-2 and other surrogates is also integral to the interpretation of surveillance data.

The goal of this study was to understand the partitioning behaviour of SARS-CoV-2, PMMoV and potential surrogates (229E, MHV) in wastewater so that methods can be improved and inform the interpretation of wastewater surveillance data. To examine viral partitioning, the RNA of these viruses in wastewater was concentrated through a series of experiments that target the separation of the liquid and solid fractions of wastewater (e.g., ultrafiltration, centrifugation, PEG precipitation). Using wastewater samples obtained in real-time during the COVID-19 pandemic from three sites in Ontario, Canada, the partitioning of SARS-CoV-2 (N1 and N2), PMMoV, and two seeded surrogates (229E, MHV) were compared under different conditions that tested low- and high-force centrifugation, PEG precipitation followed by centrifugation, and ultrafiltration devices. By employing this approach, viral partitioning was directly compared and how it was affected by the concentration methods used.

2. Materials and Methods

2.1. Collection of Wastewater

Raw wastewater influent was collected in pre-cleaned 250 mL HDPE bottles (Systems Plus, Baden, ON, Canada) from the Clarkson (Region of Peel), GE Booth (Region of Peel), and Kitchener (Region of Waterloo) wastewater treatment plants (WWTP) located in southern Ontario, Canada (general characteristics of the WWTPs are described in Table S1). Samples were then shipped to the Servos Lab at the University of Waterloo on the same day where the sample bottles were wiped with 10% (v/v) bleach, rinsed with 70% (v/v) ethanol, and exposed to ultraviolet light for 30 min to disinfect the exterior of the bottles. Samples were kept in a fridge at 4°C with experiments commencing within 1-10 days (3 days median timeframe) following collection (Table 1; visualized timeline of experiments available in the supplemental information, Figure S1). Site selection and pooling of wastewater were based on influent availability and where the SARS-CoV-2 RNA amount in wastewater was suspected to be high enough to be quantified by the concentration methods.

2.2. Concentration of Viral RNA

The surrogates, 229E and MHV, were seeded into the raw wastewater prior to the concentration step. The virus 229E was propagated on MRC-5 (ATCC CCL-171) cells (Cedarlane, Burlington, ON, Canada) and MHV (strain A59) was propagated on NCTC clone 1469 cells (derivative of NCTC 721, ATCC CCL-9.1) (Cedarlane) with additional details on cell culturing available in the supplemental information. Once harvested, both 229E and MHV were thawed from -80°C on ice, heat-inactivated for 60 min at 65°C, diluted 100-fold in qPCR water, and then placed back into a -80°C freezer until ready to be seeded into wastewater samples. As a measure to reduce variability, viral stocks of 229E and MHV were kept consistent throughout the study.

Pooled wastewater from the 250 mL collection bottles was aliquoted (40 mL) into 50 mL conical tubes and seeded with an estimate of 4.83-6.12 $\log_{10}$ copies of 229E virus and 4.57-5.33 $\log_{10}$ copies of MHV virus (Table S2) and incubated for 10 min on ice. Following the incubation, wastewater samples

6

were randomly selected for the experiments under different conditions described below at the concentration step (Figure 1).

2.2.1. Apparent Partitioning of Viral RNA

The viral partitioning of RNA of SARS-CoV-2, PMMoV, 229E, and MHV in wastewater was conducted using an approach based on centrifugation to separate wastewater into the supernatant (i.e., liquid) and pellet (i.e., solid) phases. The 40 mL wastewater aliquots were split randomly into three treatment groups to compare viral concentration methods (i.e., liquid- vs solid-based) and centrifugal force (Figure 2). The first set of tubes were centrifuged at 4,000 g for 10 min with a brake (Condition A) with the supernatant and pellets quantified as described below. The second set was centrifuged at 12,000 g for 1.5 h with no brake (Condition B) with the supernatant and pellets quantified. The final set of tubes underwent PEG precipitation (Condition C) followed by centrifugation at 12,000 g for 1.5 h without a brake and pellets (i.e., solids + liquid) quantified. Condition A (4,000 g, 10 min, with brake) was based on methods reported in the literature for SARS-CoV-2 RNA wastewater analyses tailored for liquid-based (supernatant/ultrafiltration) protocols (Ahmed et al., 2020; Chik et al., 2021; Torii et al., 2021) with the objective to quickly separate liquid and solid phases. Condition B was selected to have the same centrifugation force and time as the routine PEG precipitation protocol (Condition C) used for wastewater surveillance by the Servos Lab (Oniyebi et al., 2023a), which was partially adapted from Wu et al. (2020). Modifications to the PEG precipitation protocol by Wu et al. (2020) include the use of non-filtered wastewater and an overnight incubation step before centrifugation at 12,000 g as further described below. Moreover, centrifugation without a brake for Conditions B and Condition C was applied to improve pellet solidification.

Following incubation of the surrogate, supernatant and pellet treatments under Conditions A and Condition B proceeded to centrifugation on the same day under their respective conditions. After centrifugation, the resulting supernatant was processed with a 10 kDa molecular weight cutoff (MWCO) ultrafiltration device. Four replicates of the experiments were conducted using different ultrafiltration

7

devices (partly based on availability during the pandemic) to process the supernatant fractions. Experiments VP 1-1 (Apr. 2021) and VP 1-2 (May 2021) were conducted with an Amicon Ultra-4 device (MilliporeSigma, Oakville, ON, Canada), VP 2 (Sep. 2021) was conducted with the Amicon Ultra-15 device (MilliporeSigma), and finally, VP 3 (Jan. 2022) was conducted using the Centricon Plus-70 device (MilliporeSigma).

For each experiment, all manufacturer guidelines for the ultrafiltration devices were followed to concentrate the supernatant. Briefly, the supernatant was loaded into the ultrafiltration device, centrifuged at 4,000 g for the Amicon Ultra-4 (4 mL processed) and Amicon Ultra-15 (15 mL processed) devices and 3,500 g for the Centricon Plus-70 device (40 mL processed). A maximum of 250 μL of resulting concentrate was used for extraction of viral RNA (as described below). Viral RNA of SARS-CoV-2 in the supernatant fractions for Condition A and Condition B during VP 2 were below the dynamic range of the standard curve (1,000 to 1.6 copies/5 μL template). Therefore, only the pellet fraction and PEG precipitation/centrifugation data were included in the comparisons. Once the supernatant was transferred to the ultrafiltration device, any remaining volume of the supernatant was removed and discarded – without disturbing the pellet on the bottom – and the pellet samples were centrifuged again for another 5 min (no brake) to solidify the pellet. The remaining supernatant after centrifugation was removed using a pipette and the pellet was weighed to three decimal places. If, due to pellet sluffing, additional centrifugation was required, samples were centrifuged again for 5 min with a moderate brake. A maximum mass (wet weight) of 0.250 g of the pellet was taken for viral RNA extraction without further treatment. Obtained pellets had a mean mass (wet weight) of 0.146 (± 0.045 SD) g.

For PEG precipitation/centrifugation, following surrogate incubation, the 40 mL sample aliquots were transferred to a second set of 50 mL conical tubes containing 4 g (± 5%) PEG 8000 and 0.9 g (± 5%) NaCl (Fisher Scientific, Mississauga, ON, Canada). Next, they were vortexed at 2,000 rpm for 30 sec (Digital Vortex Mixer, Fisher Scientific), and then placed on an Advanced 3500 Orbital Shaker (VWR, Mississauga, ON, Canada) for 2 h at 150 rpm inside a 4°C fridge and incubated overnight (15-18 h). After

overnight incubation, samples were centrifuged at 12,000 *g* for 1.5 h without a brake. The supernatant was removed and discarded without disturbing the pellet on the bottom, and samples were re-centrifuged for 5 min at 12,000 *g* without a brake. Following the removal of any remaining supernatant with a pipette, a maximum mass (wet weight) of 0.250 g of the pellet was taken for viral RNA extraction. Obtained pellets had a mean mass (wet weight) of 0.169 ($\pm$ 0.021 SD) g.

2.2.2. Comparison of Ultrafiltration Devices

The ultrafiltration devices (Amicon Ultra-4, Amicon Ultra-15, and Centricon Plus-70) were compared in a head-to-head experiment (Figure 3). Wastewater (40 mL) was randomly aliquoted across 50 mL conical tubes and centrifuged using 12,000 *g* for 1.5 h without a brake to form the supernatant and pellets. While the focus was to compare the ultrafiltration devices used to concentrate viral RNA from the supernatant, the pellets were also processed for extraction of RNA (Figure S2). This experiment was replicated twice in January 2022. Both the Amicon Ultra-4 device (4 mL processed) and Ultra-15 device (15 mL processed) used the same wastewater sample tube for the liquid fraction determination. For the Centricon Plus-70 devices, all 40 mL of the supernatant was pipetted from a sample tube and loaded into the ultrafiltration device. All manufacturer guidelines were followed to concentrate the supernatant and a maximum of 250 µL of the concentrate was taken for viral RNA extraction.

2.3. Extraction of Viral RNA

Viral RNA was extracted from both pellet and supernatant concentrates following manufacturer instructions using the RNeasy PowerMicrobiome Kit (Qiagen, Germantown, MD, USA) on a QIAcube Connect instrument (Qiagen) and eluted to 100 µL in Rnase-free water. A modification of the protocol was applied to the PM1 buffer and 2-mercaptoethanol addition step by adding 100 µL of TRIzol (Fisher Scientific) to promote cell lysis before bead-beating the sample. For both replicates of VP 1, a Vortex-Genie 2 (Scientific Industries, Bohemia, New York, USA) was used for 10 min at maximum speed (3,000 rpm) to bead-beat the samples. For VP 2, VP 3, DC 1-1, and DC 1-2, a Bead Mill 24 Homogenizer

9

(Fisher Scientific) was used for 5 min at 3.55 m/s to bead-beat the samples. Preliminary testing indicated that both protocols yielded comparable viral RNA for all gene targets.

2.4. RT-qPCR

RNA extracts were quantified in triplicate by reverse transcription qPCR (qPCR) for two regions of the nucleocapsid (N) gene for endogenous SARS-CoV-2 (CDC (2020) N1 and N2) using TaqPath™ 1-Step RT-qPCR Master Mix, CG (Life Technologies, Thermo Scientific, Burlington, ON, Canada) on the CFX96 Touch or CFX Opus Real-Time PCR systems (Bio-Rad Laboratories, Hercules, CA, USA). Additionally, a region of the coat protein gene for endogenous PMMoV (Zhang et al., 2006), a region of the membrane protein gene for exogenous (seeded) 229E (Vijgen et al., 2005), and a region of the N gene for exogenous (seeded) MHV (Raaben et al., 2007) was quantified using the same master mix and qPCR instrument (see supplemental information for primer and probe sequences (MilliporeSigma) that are presented in Table S3 and cycling conditions in Table S4). SARS-CoV-2 RNA was quantified with an RNA Exact Diagnostics (EDX) SARS-CoV-2 standard (Bio-Rad Laboratories) whereas all other targets were quantified using a dsDNA gBlock standard (Integrated DNA Technologies, Coralville, IA, USA) (Table S5) with all standards verified by dPCR (QIAcuity, Qiagen, Hilden, Germany). All plates were processed with triplicates of positive controls (a standard with a known RNA concentration), non-template controls (all PCR reagents without a template), non-reverse transcriptase controls (all PCR reagents without reverse transcriptase), and standard curves with an efficiency range of 90-110%. All plates passed these quality assurance and quality control measures before commencing data analysis. Both N-gene targets and PMMoV were quantified using a simplex assay. The N-gene assay was performed in a 20 μL reaction with 5 μL of RNA template and the PMMoV assay was performed in a 10 μL reaction with 2.5 μL of RNA template. The surrogates 229E and MHV were quantified in a duplex assay performed in a 10 μL reaction with 2.5 μL of RNA template.

Finally, inhibition of reverse transcriptase and DNA polymerase was assessed with a master mix seeded with bacteriophage MS2 RNA (MilliporeSigma) and zebrafish (*Danio rerio*) DNA, respectively (gBlock,

10

IDT). Sample extracts were plated in duplicate and assessed for a one Cq shift compared to the positive control (sample replaced with Rnase-free water) to indicate qPCR inhibition (Cao et al., 2012; Swango et al., 2006). With this method, there was no indication of qPCR inhibition for the samples.

2.5. Data Analysis

An eight-point standard curve was used to quantify the samples for N1 and N2 whereas PMMoV, 229E, and MHV used a six-point standard curve. The supernatant (Equation 1) and pellet (Equation 2) fractions were then corrected for the elution volume and wastewater sample volume, as well as for pellet and liquid sub-sampling as applicable:

$$\textbf{Supernatant}_{\left(\frac{\textbf{cp}}{\textbf{40 mL}}\right)} = \frac{\textbf{cp}}{\textbf{well}} * \frac{\textbf{well}}{\textbf{template vol (}\mu\textbf{L)}} * \textbf{elution vol (}\mu\textbf{L)} * \frac{\textbf{total vol (mL)}}{\textbf{ultrafiltration vol (mL)}} * \frac{\textbf{total conc vol (}\mu\textbf{L)}}{\textbf{extracted conc vol (}\mu\textbf{L)}} * \frac{\textbf{1}}{\textbf{40 mL}} \qquad (1)$$

$$\textbf{Pellet}_{\left(\frac{\textbf{cp}}{\textbf{40 mL}}\right)} = \frac{\textbf{cp}}{\textbf{well}} * \frac{\textbf{well}}{\textbf{template vol (}\mu\textbf{L)}} * \textbf{elution vol (}\mu\textbf{L)} * \frac{\textbf{total pellet mass (g)}}{\textbf{extracted pellet mass (g)}} * \frac{\textbf{1}}{\textbf{40 mL}} \qquad (2)$$

where "cp" is the RNA copies as determined by the standard curve; "well" is the reaction well on the qPCR plate; "template vol" is the amount of template plated; "elution vol" is the volume that the PowerMicrobiome Kit eluted to in Rnase-free water; "total vol" is the total volume of the wastewater sample; "ultrafiltration vol" is the volume of supernatant loaded in the ultrafiltration device; "total conc vol" is the total volume of the concentrate post centrifugation using the ultrafiltration device; "extracted conc vol" is the amount of the concentrate that was sub-sampled into the PowerMicrobiome Kit as applicable; "total pellet mass" is the total mass of the pellet following initial centrifugation to form the pellet; and "extracted pellet mass" is the amount of the pellet that was sub-sampled into the PowerMicrobiome Kit as applicable. By dividing one fraction – the supernatant or the pellet – by the sum of both fractions (Equation 3), an estimate of the percent of viral RNA in each fraction can be calculated:

$$\textbf{Percent signal in fraction} = \frac{\textbf{copies per 40 mL}_{\textbf{fraction}}}{\textbf{copies per 40 mL}_{\textbf{pellet}} + \textbf{copies per 40 mL}_{\textbf{supernatant}}} \times \textbf{100} \qquad (3)$$

11

A one-way ANOVA was used to test if the concentration methods yielded the same log-transformed copies per 40 mL of wastewater across centrifugal conditions. In addition, a one-way ANOVA was also conducted to test for the disparity between ultrafiltration methods once corrected to log-transformed copies per 40 mL of wastewater. Following a significant ANOVA test, pairwise comparisons were made using Tukey's post-hoc test. All assumptions were reviewed including the assumption of normality (Shapiro-Wilk test and Q-Q plot) as well as the assumption of homoscedasticity (Levene's test). Finally, all statistical tests implemented a p-value threshold of 0.05 and were conducted using R version 4.0.5 (R Core Team, 2021).

3. Results

3.1. Apparent Partitioning of Viral RNA

Copies of RNA of SARS-CoV-2 (N1 and N2), PMMoV, 229E, and MHV were compared under various methods of concentration, including 4,000 *g* for 10 min with a brake (Condition A), and 12,000 *g* for 1.5 h for without a brake (Condition B), and PEG precipitation followed by centrifugation at 12,000 *g* for 1.5 h without a brake (Condition C) to examine the partitioning of these viruses. Between treatments for all targets, copies of RNA showed significant differences for the one-way ANOVA ($p < 0.017$; full results are available in the supplemental information, Table S6). Furthermore, there was a high degree of reproducibility in the observed partitioning patterns for each of the targets.

The pattern of partitioning of N1 and N2 RNA gene targets was similar within each of the experimental conditions (VP 1 to VP 3, Figure 4-6). Comparison of RNA copies of both N-gene targets between supernatant and pellets under the centrifugal condition of Condition A in VP 1-1 (Figure 4) and VP 3 (Figure 6) was significantly different (Tukey pairwise differences; $p < 0.002$) but VP 1-2 (Figure 4) was not ($p > 0.127$). Furthermore, 59-83% of the N-gene RNA signal was captured by the supernatant fraction when using Condition A. When comparing the number of copies of RNA in the supernatant relative to that in the pellet under Condition B, VP 1-1, VP 1-2, and VP 3 were not significantly different

(p > 0.810). For these experiments, the distribution of RNA between fractions ranged from 45-55%. The comparison of RNA copies of N1 and N2 between Condition A and Condition B for the same fraction generally saw non-significant Tukey differences except for three out of the 14 potential comparisons: N1 in VP 1-1 (supernatant under Condition A to supernatant under Condition B, p = 0.023); N2 in VP 1-1 (supernatant under Condition A to supernatant under Condition B, p < 0.001; and pellet under Condition A to pellet under Condition B, p = 0.043).

When the copies of N1 and N2 RNA were measured in the pellet fraction using Condition B and were compared directly to the pellet obtained after PEG precipitation followed by centrifugation at 12,000 g for 1.5 h without a brake (Condition C), the PEG precipitation treatment was on average 3.10 ± 1.12 SD fold greater among four partitioning experiments (Figure S3-S5). More specifically, the target N1 was consistently greater by a mean factor of 3.90 ± 1.08 SD whereas N2 was consistently greater by a mean factor of 2.31 ± 0.67 SD by use of PEG precipitation followed by centrifugation compared to centrifugation alone under Condition B. When concentrations of SARS-CoV-2 RNA were least during VP 2, copies of N1 RNA for PEG precipitation/centrifugation (Condition C) were 3.37-fold greater than the pellet from Condition B. Similarly, the copies of N2 RNA for PEG precipitation/centrifugation (Condition C) were 2.19-fold greater than the pellet from Condition B.

The partitioning patterns of RNA copies for PMMoV were highly reproducible in this study except in VP 2. In VP 1-1, VP 1-2 (Figure 4) and VP 3 (Figure 6), the RNA copies of PMMoV for the supernatant treatments between Condition A and Condition B had non-significant Tukey pairwise comparisons (0.075 < p < 0.985). For the RNA copies of PMMoV for the pellet treatments between Condition A and Condition B, there were also non-significant Tukey differences (0.060 < p < 0.220). The RNA copies measured in the supernatant for PMMoV ranged from 65-91% of the total signal in the sample across all experiments. However, of this range, the percent of RNA copies of PMMoV in the supernatant during VP 2 was lowest for both Condition A and Condition B at 76% and 65%, respectively. Together, these two

13

lower measurements during VP 2 added to the variability of PMMoV RNA measured in the supernatant. Otherwise, >78% of PMMoV RNA was measured in the supernatant when excluding VP 2.

Overnight PEG precipitation followed by centrifugation at 12,000 g for 1.5 h without a brake (Condition C) had a greater number of copies of PMMoV RNA than the pellets without PEG precipitation but less than the number of copies of RNA that were in the supernatant that was measured by ultrafiltration devices from either Condition A or Condition B (Figure 4-6). However, in VP 2 (Figure 5) RNA copies of PMMoV in the supernatant fractions under Condition A and Condition B were not significantly different than the PEG precipitation treatment (p > 0.565), which was different from VP 1-1, VP 1-2, and VP 3. Finally, the number of copies of RNA collected by use of PEG precipitation followed by centrifugation (Condition C) were on average 1.97-fold ± 0.24 SD greater than the pellet treatment under the same centrifuge conditions of 12,000 g for 1.5 h without a brake (Figure S3-S5) among the three experiments.

In general, patterns of partitioning of RNA of the surrogates 229E and MHV were similar among all partitioning conditions. However, there was variability with what centrifugal conditions were determined to be significantly different. For VP 1-1, VP 1-2 (Figure 4), and VP 3 (Figure 6), the copies of RNA of the surrogates centrifuged under Condition A were enriched in the supernatant fraction. For 229E, copies of RNA in the supernatant ranged from 81-97% and for MHV, copies of RNA in the supernatant fraction ranged from 61-92%. The Tukey pairwise comparisons between the supernatant and pellet treatments were significant for VP 1-1, VP 1-2, and VP 3 (p < 0.009). In VP 2 (Figure 5), the RNA copies in the supernatant treatment were less than the RNA copies in the pellet treatment for both 229E (p < 0.001) and MHV (p < 0.001) and only comprised 25% and 15% of the total amount of RNA, respectively.

Precipitation by use of PEG followed by centrifugation at 12,000 g for 1.5 h without a brake (Condition C) had greater RNA copies of 229E and MHV than the pellet treatment under Condition B. There was an average factor of 1.44 ± 0.27 more RNA copies of 229E with PEG precipitation than the pellets processed without PEG precipitation under the shared centrifugal condition (Figure S3-S5).

14

Similarly, for RNA copies of MHV, there was an observed increase by a factor of 1.42 ± 0.35 when PEG precipitation was used (Condition C) than the pellet treatment under Condition B. Despite these average increases, only VP 1-1 (Figure 4) showed significant Tukey differences for the RNA copies between the pellet treatment under Condition B and PEG precipitation followed by centrifugation (Condition C) for both 229E ($p = 0.039$) and MHV ($p = 0.010$). Here, the observed increase by PEG precipitation followed by centrifugation (Condition C) was 1.73-fold and 1.68-fold, respectively.

3.2. Comparisons of Ultrafiltration Devices

Numbers of copies of RNA of N1, N2, PMMoV, 229E and MHV were compared using the Amicon Ultra-4, Amicon Ultra-15, and Centricon Plus-70 devices. Generally, there was good reproducibility between the ultrafiltration devices (Figure 7). The comparison of RNA copies between treatments (ultrafiltration devices) for all targets showed significant differences for the one-way ANOVA test ($p < 0.001$; full results are available in the supplemental information, Table S7). There was a consistent observation across all targets that the Amicon Ultra-15 device had the lowest RNA copies, and the Centricon Plus-70 device had the greatest number of copies of RNA. The three ultrafiltration devices selected for this study suggest excellent reproducibility but did not provide equivalent estimates (Figure 7). For all targets, the Amicon Ultra-4 device and the Centricon Plus-70 device quantified copies of RNA similarly, but the Centricon Plus-70 had marginally better performance. This pattern was observed in both experiments of the ultrafiltration device comparisons (Figure 7).

The Amicon Ultra-15 and Centricon Plus-70 devices had similar RNA copies of N1 and N2 during both ultrafiltration device comparison experiments; DC 1-1 and DC 1-2 (Figure 7). The number of copies of RNA of N2 in DC 1-1 was the only comparison of the N-gene targets to have a non-significant pairwise comparison ($p = 0.450$) between the Amicon Ultra-4 and the Centricon Plus-70 devices. Accordingly, the RNA copies of N2 in DC 1-2 and N1 in both DC 1-1 and DC 1-2 were significantly different ($p < 0.033$). The difference between the mean number of copies of RNA for the Amicon Ultra-4 and Centricon Plus-70 devices of N1 in DC 1-1 was 0.20 log RNA copies ($p = 0.033$) versus 0.14 log

15

RNA copies of N2 (p = 0.450). In DC 1-2, the log difference between means was 0.49 copies (p < 0.001) and 0.27 copies (p = 0.014) of N1 and N2, respectively. The Amicon Ultra-15 device had lesser measured concentrations of both N-gene comparisons (p < 0.002) compared to either the Amicon Ultra-4 or the Centricon Plus-70 devices.

Copies of PMMoV RNA had the same pattern for both replicates of the ultrafiltration device comparison; DC 1-1 and DC 1-2 (Figure 7). First, copies of PMMoV RNA for the Amicon Ultra-4 and Centricon Plus-70 devices were not significantly different (Tukey's post hoc test; p = 0.265) for DC 1-1 and DC 1-2 (p = 0.620). Additionally, copies of PMMoV RNA for the Amicon Ultra-15 device were significantly different for Tukey's post-hoc comparison than both the Amicon Ultra-4 and Centricon Plus-70 devices (p < 0.001) for both replicates (DC 1-1 and DC 1-2). Overall, copies of PMMoV RNA measured by the three ultrafiltration devices were reproducible between DC 1-1 and DC 1-2. Moreover, the Amicon Ultra-15 device consistently had fewer copies of RNA of PMMoV compared to the Amicon Ultra-4 and Centricon Plus-70 devices.

Patterns of partitioning of RNA copies of the surrogates 229E and MHV were consistent with results observed for N1, N2, and PMMoV (Figure 7). Tukey's pairwise comparisons for 229E were significantly different for all combinations of ultrafiltration devices in DC 1-1 and DC 1-2 (p < 0.024). Copies of RNA of 229E for the Amicon Ultra-4 device were closer to the Centricon Plus-70 device in DC 1-1 (p = 0.016) and DC 1-2 (p = 0.024) than it was against its Amicon Ultra-15 device counterpart (p < 0.001) for both replicates (DC 1-1 and DC 1-2). The comparison for the RNA copies of MHV for the Amicon Ultra-4 and Centricon Plus-70 devices was similar between DC 1-1 and DC 1-2. In DC 1-1, the comparison was not significantly different (p = 0.054) but in DC 1-2 it was (p = 0.050). Similar to 229E and the other targets (N1, N2, PMMoV), the Amicon Ultra-15 device gave consistently lesser concentrations of MHV than both the Amicon Ultra-4 and Centricon Plus-70 devices in both replicates of the ultrafiltration device comparison (p < 0.001).

4. Discussion

16

4.1. Apparent Partitioning of Viral RNA

Understanding the apparent partitioning of viruses in wastewater is important to ensure a more informed interpretation of SARS-CoV-2 trends in wastewater. Since N1 and N2 are sequences on the N-gene, it is expected that they would provide equivalent results among varied centrifugal conditions. Like this study, Kim et al. (2022) noted that amounts of N1 and N2 were correlated in both the liquid and solid fractions of wastewater. For the surrogates, copies of RNA of 229E and MHV were also evenly distributed under Condition B (12,000 g, 1.5 h, without brake). However, unlike SARS-CoV-2, copies of RNA of 229E and MHV tended to partition further to the supernatant fraction under Condition A (4,000 g, 10 min, with brake), which indicated that under this condition the surrogates behaved differently. This observation has also been observed by others (Chik et al., 2021; Hasing et al., 2021). Since the surrogates are seeded into the wastewater sample, it is possible they will not associate with the solids as readily as exogenous SARS-CoV-2 given that SARS-CoV-2 is predominantly transported into wastewater through excreted feces (Chik et al., 2021; Hasing et al., 2021). However, the methods described here separate the liquid and solid phases differently, using centrifugation (3,000-12,000 g), filtration (22 μm or 45 μm), gravitational settling, or a combination of these techniques. Accordingly, these methods might then have inherent differences in the way they determine apparent partitioning as described by this study. Moreover, as surrogates handling can vary, either through inactivation or spike duration, these may affect the partitioning of the surrogates (Chik et al., 2021; Sinclair et al., 2012).

Contrary to SARS-CoV-2 (i.e., N1 and N2), PMMoV had a different pattern among partitioning conditions. The centrifugal condition had a minimal or no effect on recoveries of PMMoV in each phase. Regardless of conditions, RNA copies of PMMoV remained primarily in the supernatant fraction (65-91%). Since PMMoV is ubiquitous in wastewater (Kitajima et al., 2018), it has been widely used to normalize the SARS-CoV-2 signal to improve trends over time by accounting for the apparent variability in fecal content among samples of wastewater (D'Aoust et al., 2021; Wu et al., 2020). However, the apparent differences in partitioning of PMMoV and SARS-CoV-2 do raise further questions about its

17

application as an endogenous reference to normalize SARS-CoV-2. It has also been shown that PMMoV

RNA can persist in wastewater longer than SARS-CoV-2 RNA at varying temperatures (4, 12, or 20°C)

with this observation exacerbated in the liquid (solids removed) fraction (Burnet et al., 2023). Therefore,

it is possible that under some conditions, normalizing the SARS-CoV-2 wastewater signal with PMMoV

might result in greater variability (Burnet et al., 2023). Moreover, the differences in the apparent

partitioning of PMMoV in the liquid fraction compared to SARS-CoV-2 might also resulted in additional

variability as the fate of the two viruses might differ.

The observation that the addition of overnight PEG precipitation followed by centrifugation (12,000

g, 1.5 h, without brake) increased the concentration detected in the pellet by 3.10-fold relative to the

similar condition without PEG precipitation (Figure S3-S5), suggests it is possible to increase the yield of

SARS-CoV-2 RNA in a pellet fraction by increasing the centrifugal force or addition of chemicals to

facilitate aggregation and precipitation of the solids/colloids. This is achieved through the reduction of

solvent (i.e., water) availability thereby promoting an environment for organic matter or genetic material

to be displaced and pelleted more readily (Atha & Ingham, 1981; Poison, 1977). Studies that have

compared the direct capture of the solids against PEG precipitation followed by centrifugation often have

different centrifugal conditions and may also first remove solids before PEG precipitation (Kaya et al.,

2022; LaTurner et al., 2021; Pecson et al., 2021). As a result, it is challenging to discern differences

between the use of PEG precipitation and a solids-only approach as the underlying centrifugation

conditions can differ. Some studies have noted PEG precipitation followed by centrifugation to be poor

for enveloped viruses (Kitamura et al., 2021; Ye et al., 2016) while it has also been found to be effective

(Barril et al., 2021; Kaya et al., 2022). Interestingly, following a low-force solid removal step, PEG

precipitation has been shown to have a higher recovery of enveloped viruses over ultrafiltration with the

opposite also being observed (Ahmed et al., 2020; Kaya et al., 2022). By comparing PEG precipitation

without the removal of solids to a solids-only approach under the same centrifugal condition (12,000 *g*,

1.5 h, no brake), it is clear that PEG precipitation improves overall SARS-CoV-2 RNA recovery.

Moreover, under the conditions of this study, PEG precipitation had a higher recovery of SARS-CoV-2 RNA over ultrafiltration with the three devices evaluated. During periods of low SARS-CoV-2 concentration in wastewater, such as the period during VP 2 (Figure 5; Figure S1), use of both fractions of wastewater can achieve higher recovery which might allow for more reliable trends since detection limit concerns are partially mitigated.

There is a consensus that SARS-CoV-2 should partition to the solids, assuming the virus is intact, due to its enveloped structure (Ahmed et al., 2020; Kitamura et al., 2021) because the lipid bilayer provides lipophilic characteristics (Gundy et al., 2008; Schoeman & Fielding, 2019). Using two enveloped viruses, MHV and *Pseudomonas* phage ϕ6, and two non-enveloped viruses, *Enterobacteria* phage MS2 and T3, Ye et al. (2016) showed that seeded enveloped viruses adsorbed to the solid fraction in wastewater in greater proportion than the seeded nonenveloped viruses when the solids were removed from the wastewater using a centrifugal condition of 30,000 g for 10 min. With this condition, a maximum of 26% of the enveloped viruses were determined to adsorb to the solid fraction while nonenveloped viruses were estimated to have a maximum of 6% adsorb to solids (Ye et al., 2016). However, adoption of solid-based approaches fails to recognize that a major proportion of the viral signal might remain in the liquid phase of the wastewater as demonstrated by this study and by others (Chik et al., 2021; Hasing et al., 2021).

To add to these adsorption considerations, Wellings (1976) noted that viruses are part of the solid fraction through both adsorption and being integrally part of the solids (i.e., embedded) and that methods often fail to recognize the latter. With the virus embedded in feces or adsorbed to organic matter, it has been suggested that this might act as a form of protection from degradation (Gundy et al., 2008; Rahimi et al., 2021). It has also been documented that DNA adsorbed to soil colloids and minerals was protected from degradation from DNases (Cai et al., 2006). Therefore, it is plausible that RNA in the liquid phase is adsorbed to colloidal material and shielded from degradation in wastewater. Thus, ultrafiltration would capture the colloidal material along with SARS-CoV-2 RNA and other viruses that might be adsorbed to the aforementioned colloidal material. However, clogging or membrane adsorption may be a concern

19

(Ahmed et al., 2020). In summary, it is improbable that the RNA being measured in the wastewater is not protected from RNases in the wastewater in some form.

Correspondingly, this explains why cooled samples can be held for many days, such as the wastewater used for VP 3 and DC 1-1 in this study, without a major shift in the SARS-CoV-2 signal (Hokajärvi et al., 2021; Islam et al., 2022; Simpson et al., 2021). While partitioning patterns were consistent in this study, as measured during different waves of the COVID-19 pandemic (Figure S1), the effect of storage conditions on viral partitioning requires further investigation. Furthermore, partitioning could be measured over time after a virus has been seeded into a wastewater matrix as previously described by Fauvel et al. (2017) using F-specific RNA bacteriophages. Such an approach may elucidate the partitioning kinetics of SARS-CoV-2 and other viruses of public health significance in wastewater. With this in mind, it would be important to consider the phase separation methodology as that might affect how partitioning patterns are measured.

As previously mentioned, there has been a strong emphasis in the literature on solid-based approaches for measuring SARS-CoV-2 RNA in wastewater (Chik et al., 2021; D'Aoust et al., 2021; Graham et al., 2021; Kim et al., 2022; Kitamura et al., 2021). Commonly, partitioning results are reported on a concentration basis (e.g., copies/mL or copies/g) that makes the solid fraction appear more important (Graham et al., 2021; Kim et al., 2022) even though the largest portion of the virus might remain in the liquid/colloidal phase. Based on the total copies in each phase, it is evident that SARS-CoV-2 exists almost equally between the supernatant and pellet fractions under 12,000 g for 1.5 h without a brake. To only target and quantify the solid fraction eliminates at least half of the RNA signal if conditions are similar to those used by this study. Therefore, this study supports that although SARS-CoV-2 enriches in the solid fraction due to a substantially lower solids-to-liquid ratio in the wastewater, a large proportion (approximately 50-80%), remains in the supernatant fraction (depending on the conditions). It is likely that SARS-CoV-2 RNA is associated with very small particles or colloidal material that does not settle during centrifugation.

It is still unknown if the SARS-CoV-2 virus remains intact, fragmented, or degraded in wastewater by the time it reaches the concentration step in the quantification process (Graham et al., 2021; Hill et al., 2021; LaTurner et al., 2021). In addition, concentration methods, such as PEG precipitation, might also affect the structure of viruses as PEG and NaCl have been documented to degrade the lipid bilayer (Boni et al., 1981; Cordova et al., 2003). Based on correlative light fluorescence and electron microscopy, at least some intact SARS-CoV-2 virus might exist in wastewater (Belhaouari et al., 2021). Moreover, using integrity-based qPCR, it has been suggested that several forms of SARS CoV-2 could exist in wastewater based on experiments that seeded infectious SARS-CoV-2 into wastewater (Wurtzer et al., 2021). Although the intact virus might exist in wastewater, it may remain noninfective due to enzymatic modifications to the spike protein in the digestive tract before being shed into sewer systems (Robinson et al., 2022). It is unlikely that fully intact SARS-CoV-2 virus exists in wastewater, but the RNA might also be shielded by ribonucleoprotein complexes (Monda' et al. 2021) and therefore protected from rapid degradation in the wastewater. It is therefore likely that a combination of mostly intact and fragmented SARS-CoV-2 RNA exists in wastewater that is both adsorbed to and embedded within the solids.

4.2. Comparisons of Ultrafiltration Devices

Direct comparison of the three ultrafiltration devices (Amicon Ultra-4, Amicon Ultra-15, and Centricon Plus-70) showed that they had different abilities to isolate SARS-CoV-2, PMMoV, and the seeded surrogates (229E, MHV) (Figure 7). Supply chain challenges experienced throughout this study limited the availability of different devices during the viral partitioning experiments (VP 1 to VP 3) which made it necessary to compare their performance directly. Although these devices have been used in other methods and compared indirectly as part of interlaboratory studies (Chik et al., 2021; Pecson et al., 2021), a direct comparison of all three devices had not been reported previously. However, there have been some comparisons between the Amicon Ultra-15 and the Centricon Plus-70 devices.

Ahmed et al. (2020) compared seeded MHV concentrations using various ultrafiltration brands with different membrane sizes: a 30 kDa MWCO Amicon Ultra-15 device and a 10 kDa MWCO Centricon

Plus-70 device. The pre-filtration step, which forms the pellet, used a centrifugal force of 4,500 g for 10 min, which is similar to the Condition A applied in the current study, resulted in a 30% loss of MHV when comparing the ultrafiltration devices (Ahmed et al., 2020). Furthermore, depending on the ultrafiltration device used, such as the Amicon Ultra-15 or Centricon Plus-70 devices, as well as the MWCO of 10 kDa or 100 kDa, and the RNA extraction kit used, Kaya et al. (2022) demonstrated that under a 3,400 g spin for 15 min, liquid-based approaches had a 1.7-48.8 percent point increase of the enveloped virus, bovine respiratory syncytial virus (BRSV), over a solids-only approach. Correspondingly, these data are consistent with the data presented here since SARS-CoV-2, 229E, and MHV were primarily in the supernatant fraction under a moderate centrifugal condition (i.e., Condition A).

In contrast to this study, the Amicon Ultra-15 device has been shown to perform better than the Centricon Plus-70 (Ahmed et al., 2020; Kaya et al., 2022). With inhibition not present in either study, which minimizes concern about co-concentration of inhibitors, the loss could be due to adsorption to the membrane due to a greater surface area for the Centricon Plus-70 device (Ahmed et al., 2020; Ikner et al., 2012; Kaya et al., 2022). However, the design of the Centricon Plus-70 device might have greater RNA yields for the studied gene targets over the Amicon devices as it enables the user to capture more of the particulate matter when the concentrate cup is inverted to collect the concentrate. Between the two experiments that compared ultrafiltration devices (Figure 7), the surrogates (229E, MHV) suggested that the Amicon Ultra-15 device underestimated viral RNA compared to the Amicon Ultra-4 and Centricon Plus-70 devices. Comparatively, this was in line with what was also observed with SARS-CoV-2 and PMMoV. Such as the case with VP 2, this would suggest that the poor recovery for SARS-CoV-2 was in part due to the performance of the Amicon Ultra-15 device, as well as it being a period where clinical cases and SARS-CoV-2 RNA concentrations in wastewater were already low (Figure S1). With a method reliant on the Amicon Ultra-15 device, there is a risk that surveillance data for public health might be biased by the poorer performance of the device; at least under the conditions used in this study, since it

may estimate less than the actual concentrations of SARS-CoV-2 RNA in wastewater. Overall, there is evidence that ultrafiltration devices do not quantify viral RNA equivalently (Figure 7) and great care should be taken to thoroughly test and optimize the methods used.

There are a few limitations to consider when comparing ultrafiltration devices. First, differences in membrane size should be tested as the 10 kDa MWCO can clog more readily. Depending on the matrix, this could be a factor to deal with when filtering with the devices. Testing different membrane sizes against each other would clarify if they can be used interchangeably (i.e., if a MWCO of 10 kDa garners comparable results as 30 kDa). For SARS-CoV-2, membranes with pores as small as 10 kDa MWCO have performed marginally better than those with a larger MWCO of 100 kDa (Boogaerts et al., 2021). However, with BRSV, Kaya et al. (2022) reported that the 100 kDa MWCO performed better than 10 kDa MWCO. For the Amicon Ultra-4 device, the surface area to process volume ratio is 0.75 (3 cm^2:4 mL) whereas the Amicon Ultra-15 device has a ratio of 0.51 (7.6 cm^2:15 mL). With a smaller surface area to process volume ratio, there might be an increased tendency to clog and trap RNA associated with particles that should otherwise remain in the concentrate. Nonetheless, further testing should be done to verify these comparisons for viruses measured in wastewater.

5. Conclusion

In conclusion, partitioning of SARS-CoV-2 and related viruses is not constant, but rather a function of the concentration method, and therefore more appropriately described as apparent partitioning. RNA of SARS-CoV-2 showed an even split between the supernatant and pellet fractions under centrifugal conditions that are moderately strong and long (12,000 *g*, 1.5 h, no brake). The implication of this is that a diverse suite of methods can quantify SARS-CoV-2 since it is present in both fractions. Additionally, care must be taken when selecting ultrafiltration devices as they are not equivalent and might underestimate viral RNA in the supernatant fraction under some conditions. Since PMMoV is morphologically different than SARS-CoV-2, and there is a difference in its apparent partitioning, it is recommended that care be taken with its use as a normalizer. Accordingly, further research is required to better characterize the

partitioning kinetics of SARS-CoV-2 and related viruses in wastewater so methods can continue to be developed. Such research would address where these viruses are located in wastewater (i.e., adsorbed, embedded, or in solution) and if the viruses are intact, fragmented, or degraded before extracting them. The viruses 229E and MHV can be effective surrogates for SARS-CoV-2, although care must be taken to consider the apparent partitioning of the surrogates to ensure it aligns more closely with SARS-CoV-2 in the selected analytical approach. Another key strength of using surrogates is benchmarking a method's performance and to flag potential inconsistencies. Finally, it is recommended that WBS programs reflect on the strengths and limitations of diverse methods to establish a foundation of best practices. Understanding the behaviour of viruses and surrogates is critical to the development of robust methods and interpretation of results and will help prepare for WBS applications to other emerging infectious diseases of concern.

Declaration of Competing Interest

The authors declare that they have no known competing financial interests or personal relationships that could have appeared to influence the work reported in this paper.

Funding Sources

Projects for Public Welfare Research Institutes, National Key Research and Development Program (Grant No. 2022YFC3902103) (YX).

Data Availability

The raw data that supports the conclusions of this article has been deposited in the Federated Research Data Repository (FRDR) and is available at: https://doi.org/10.20383/102.0747. Additional questions regarding the data can be made to MS.

Acknowledgements

References

Aguiar-Oliveira, M. de L., Campos, A., R. Matos, A., Rigotto, C., Sotero-Martins, A., Teixeira, P. F. P., & Siqueira, M. M. (2020). Wastewater-based epidemiology (WBE) and viral detection in polluted surface water: A valuable tool for COVID-19 surveillance—A brief review. *International Journal of Environmental Research and Public Health*, *17*(24), 9251. https://doi.org/10.3390/ijerph17249251

Ahmed, W., Bertsch, P. M., Bivins, A., Bibby, K., Farkas, K., Gathercole, A., Haramoto, E., Gyawali, P., Korajkic, A., McMinn, B. R., Mueller, J. F., Simpson, S. L., Smith, W. I. M., Symonds, E. M., Thomas, K. V, Verhagen, R., & Kitajima, M. (2020). Comparison of virus concentration methods for the RT-qPCR-based recovery of murine hepatitis virus, a surrogate for SARS-CoV-2 from untreated wastewater. *Science of The Total Environment*, *739*, 139960. https://doi.org/10.1016/j.scitotenv.2020.139960

Ai, Y., Davis, A., Jones, D., Lemeshow, S., Tu, H, He, F., Ru, P., Pan, X., Bohrerova, Z., & Lee, J. (2021). Wastewater SARS-CoV-2 monitoring as a community-level COVID-19 trend tracker and variants in Ohio, United States. *Science of the Total Environment*, *801*, 149757. https://doi.org/10.1016/j.scitotenv.2021.149757

Artika, I. M., Dewantari, A. K., & Wiyatno, A. (2020). Molecular biology of coronaviruses: Current knowledge. *Heliyon*, *6*(8), e04743. https://doi.org/10.1016/j.heliyon.2020.e04743

Atha, D. H., & Ingham, K. C. (1981). Mechanism of precipitation of proteins by polyethylene glycols: Analysis in terms of excluded volume. *Journal of Biological Chemistry*, *256*(23), 12108–12117. https://doi.org/10.1016/S0021-9258(18)43240-1

Barril, P. A., Pianciola, L. A., Mazzeo, M., Ousset, M. J., Jaureguiberry, M. V., Alessandrello, M., Sánchez, G., & Oteiza, J. M. (2021). Evaluation of viral concentration methods for SARS-CoV-2 recovery from wastewaters. *Science of the Total Environment*, *756*, 144105. https://doi.org/10.1016/j.scitotenv.2020.144105

Belhaouari, D. B., Wurtz, N., Grimaldier, C., Lacoste, A., Pires de Souza, G. A., Penant, G., Hannat, S., Baudoin, J.-P., & La Scola, B. (2021). Microscopic observation of SARS-like particles in RT-qPCR SARS-CoV-2 positive sewage samples. *Pathogens*, *10*(5), 516. https://doi.org/10.3390/pathogens10050516

Boni, L. T., Stewart, T. P., Alderfer, J. L., & Hui, S. W. (1981). Lipid-polyethylene glycol interactions: II. Formation of defects in bilayers. *The Journal of Membrane Biology*, *62*(1–2), 71–77. https://doi.org/10.1007/BF01870201

Boogaerts, T., Jacobs, L., De Roeck, N., Van den Bogaert, S., Aertgeerts, F., Lahousse, L., van Nuijs, A. L. N., & Delputte, P. (2021). An alternative approach for bioanalytical assay optimization for wastewater-based epidemiology of SARS-CoV-2. *Science of the Total Environment*, *789*, 148043. https://doi.org/10.1016/j.scitotenv.2021.148043

Burnet, J.-B., Cauchie, H.-M., Walczak, C., Goedes, N., & Ogorzaly, L. (2023). Persistence of endogenous RNA biomarkers of SARS-CoV-2 and PMMoV in raw wastewater: Impact of temperature and implications for wastewater-based epidemiology. *Science of The Total Environment*, *857*, 159401. https://doi.org/10.1016/j.scitotenv.2022.159401

Cai, P., Huang, Q. Y., & Zhang, X. W. (2006). Interactions of DNA with clay minerals and soil colloidal particles and protection against degradation by DNase. *Environmental Science and Technology*, *40*(9), 2971–2976. https://doi.org/10.1021/es0522985

Cao, Y., Griffith, J. F., Dorevitch, S., & Weisberg, S. B. (2012). Effectiveness of qPCR permutations, internal controls and dilution as means for minimizing the impact of inhibition while measuring *Enterococcus* in environmental waters. *Journal of Applied Microbiology*, *113*(1), 66–75. https://doi.org/10.1111/j.1365-2672.2012.05305.x

Centers for Disease Control and Prevention. (2020, April 10). *Research use only 2019-novel coronavirus (2019-nCoV) real-time RT-PCR primer and probe information*. Retrieved December 13, 2022, from

https://web.archive.org/web/20200506150010/https://www.cdc.gov/coronavirus/2019-ncov/lab/rt-pcr-panel-primer-probes.html

Chik, A. H. S., Glier, M. B., Servos, M., Mangat, C. S., Pang, X.-L., Qiu, Y., D'Aoust, P. M., Burnet, J.-B., Delatolla, R., Dorner, S., Geng, Q., Giesy, J. P., McKay, R. M., Mulvey, M. R., Prystajecky, N., Srikanthan, N., Xie, Y., Conant, B., & Hrudey, S. E. (2021). Comparison of approaches to quantify SARS-CoV-2 in wastewater using RT-qPCR: Results and implications from a collaborative inter-laboratory study in Canada. *Journal of Environmental Sciences*, *107*, 218–229. https://doi.org/10.1016/j.jes.2021.01.029

Cordova, A., Deserno, M., Gelbart, W. M., & Ben-Shaul, A. (2003). Osmotic shock and the strength of viral capsids. *Biophysical Journal*, *85*(1), 70–74. https://doi.org/10.1016/S0006-3495(03)74455-5

D'Aoust, P. M., Mercier, E., Montpetit, D., Jia, J. J., Alexandrov, I., Neault, N., Baig, A. T., Mayne, J., Zhang, X., Alain, T., Langlois, M. A., Servos, M. R., MacKenzie, M., Figeys, D., MacKenzie, A. E., Graber, T. E., & Delatolla, R. (2021). Quantitative analysis of SARS-CoV-2 RNA from wastewater solids in communities with low COVID-19 incidence and prevalence. *Water Research*, *188*, 116560. https://doi.org/10.1016/j.watres.2020.116560

Dhiyebi, H., Cheng, L., Varia, M., Atanas, K., Srikanthan, N., Hayat, S., Ikert, H., Fuzzen, M., Sing-Judge, C., Badlani, Y., Zeeb, E., Bragg, L., Delatolla, R., Giesy, J., Gilliland, E., & Servos, M. (2023a). Estimation of COVID-19 case incidence during the Omicron outbreaks based on SARS-CoV-2 wastewater load in previous waves, Peel Region, Canada. *Emerging Infectious Diseases [in review]*.

Dhiyebi, H., Farah, J. A., Ikert, H., Srikanthan, N., Hayat, S., Bragg, L., Qasim, A., Payne, M., Kaleis, L., Paget, C., Celmer-Repin, D., Folkema, A., Drew, S., Delatolla, R., Giesy, J. P., & Servos, M. R. (2023b). Assessment of seasonality and normalization techniques for wastewater-based surveillancein Ontario, Canada. *Frontiers in Public Health [in review]*.

Fauvel, B., Ogorzaly, L., Cauchie, H.-M., & Gantzer, C. (2017). Interactions of infectious F-specific RNA bacteriophages with suspended matter and sediment: Towards an understanding of FRNAPH distribution in a river water system. *Science of The Total Environment*, *574*, 960–968. https://doi.org/10.1016/j.scitotenv.2016.09.115

Feng, S., Roguet, A., McClary-Gutierrez, J. S., Newton, R. J., Kloczko, N., Meiman, J. G., & McLellan, S. L. (2021). Evaluation of sampling, analysis, and normalization methods for SARS-CoV-2 concentrations in wastewater to assess COVID-19 burdens in Wisconsin communities. *ACS ES&T Water*, *1*(8), 1955–1965. https://doi.org/10.1021/acsestwater.1c00160

Graham, K. E., Loeb, S. K., Wolfe, M. K., Catoe, D., Sinnott-Armstrong, N., Kim, S., Yamahara, K. M., Sassoubre, L. M., Mendoza Grijalva, L. M., Roldan-Hernandez, L., Langenfeld, K., Wigginton, K. R., & Boehm, A. B. (2021). SARS-CoV-2 RNA in wastewater settled solids is associated with COVID-19 cases in a large urban sewershed. *Environmental Science and Technology*, *55*(1), 488–498. https://doi.org/10.1021/acs.est.0c06191

Gundy, P. M., Gerba, C. P., & Pepper, I. L. (2008). Survival of coronaviruses in water and wastewater. *Food and Environmental Virology*, *1*(1), 10. https://doi.org/10.1007/s12560-008-9001-6

Hasing, M., Yu, J., Qiu, Y., Maal-bared, R., Bhavanam, S., Lee, B., Hrudey, S., & Pang, X. (2021). Comparison of detecting and quantitating SARS-CoV-2 in wastewater using moderate-speed centrifuged solids versus an ultrafiltration method. *Water*, *13*(16), 2166. https://doi.org/10.3390/w13162166

Hill, K., Zamyadi, A., Deere, D., Vanrolleghem, P. A., & Crosbie, N. D. (2021). SARS-CoV-2 known and unknowns, implications for the water sector and wastewater-based epidemiology to support national responses worldwide: Early review of global experiences with the COVID-19 pandemic. *Water Quality Research Journal*, *56*(2), 57–67. https://doi.org/10.2166/wqrj.2020.100

Hokajärvi, A. M., Rytkönen, A., Tiwari, A., Kauppinen, A., Oikarinen, S., Lehto, K. M., Kankaanpää, A.,

Gunnar, T., Al-Hello, H., Blomqvist, S., Miettinen, I. T., Savolainen-Kopra, C., & Pitkänen, T. (2021). The detection and stability of the SARS-CoV-2 RNA biomarkers in wastewater influent in Helsinki, Finland. *Science of the Total Environment*, *770*, 145274. https://doi.org/10.1016/j.scitotenv.2021.145274

Hrudey, S. E., Bischel, H. N., Charrois, J., Chik, A. H. S., Conant, B., Delatolla, R., Dorner, S., Graber, T., Hubert, C., Isaac-Renton, J., Pons, W., Safford, H., Servos, M., & Sikora, C. (2022). *Wastewater Surveillance for SARS-CoV-2 RNA in Canada (August 2022)*. Royal Society of Canada. https://rsc-src.ca/en/covid-19-policy-briefing/wastewater-surveillance-for-sars-cov-2-rna-in-canada

Ikner, L. A., Gerba, C. P., & Bright, K. R. (2012). Concentration and recovery of viruses from water: A comprehensive review. *Food and Environmental Virology*, *4*(2), 41–67. https://doi.org/10.1007/s12560-012-9080-2

International Committee on Taxonomy of Viruses. (2021, July). *Virus Taxonomy: 2021 release, EC 53*. Retrieved January 27, 2023, from https://ictv.global/taxonomy

Islam, G., Gedge, A., Lara-Jacobo, L., Kirkwood, A., Simmons, D., & Desaulniers, J. P. (2022). Pasteurization, storage conditions and viral concentration methods influence RT-qPCR detection of SARS-CoV-2 RNA in wastewater. *Science of the Total Environment*, *821*, 153228. https://doi.org/10.1016/j.scitotenv.2022.153228

Kaya, D., Niemeier, D., Ahmed, W., & Kjellerup, B. V. (2022). Evaluation of multiple analytical methods for SARS-CoV-2 surveillance in wastewater samples. *Science of The Total Environment*, *808*, 152033. https://doi.org/10.1016/j.scitotenv.2021.152033

Kim, S., Kennedy, L. C., Wolfe, M. K., Criddle, C. S., Duong, D. H., Topol, A., White, B. J., Kantor, R. S., Nelson, K. L., Steele, J. A., Langlois, K., Griffith, J. F., Zimmer-Faust, A. G., McLellan, S. L., Schussman, M. K., Ammerman, M., Wigginton, K. R., Bakker, K. M., & Boehm, A. B. (2022). SARS-CoV-2 RNA is enriched by orders of magnitude in primary settled solids relative to liquid

wastewater at publicly owned treatment works. *Environmental Science: Water Research and Technology*, *8*(4), 757–770. https://doi.org/10.1039/d1ew00826a

Kitajima, M., Sassi, H. P., & Torrey, J. R. (2018). Pepper mild mottle virus as a water quality indicator. *npj Clean Water*, *1*(1). https://doi.org/10.1038/s41545-018-0019-5

Kitamura, K., Sadamasu, K., Muramatsu, M., & Yoshida, H. (2021). Efficient detection of SARS-CoV-2 RNA in the solid fraction of wastewater. *Science of the Total Environment*, *763*, 144587. https://doi.org/10.1016/j.scitotenv.2020.144587

La Rosa, G., Bonadonna, L., Lucentini, L., Kenmoe, S., & Suffredini, E. (2020). Coronavirus in water environments: Occurrence, persistence and concentration methods - A scoping review. *Water Research*, *179*, 115899. https://doi.org/10.1016/j.watres.2020.115899

LaTurner, Z. W., Zong, D. M., Kalvapalle, P., Gamar, K. R., Terwilliger, A., Crosby, T., Ali, P., Avadhanula, V., Santos, H. H., Weesner, K., Hopkins, L., Piedra, P. A., Maresso, A. W., & Stadler, L. B. (2021). Evaluating recovery, cost and throughput of different concentration methods for SARS-CoV-2 wastewater-based epidemiology. *Water Research*, *197*, 117043. https://doi.org/10.1016/j.watres.2021.117043

Manuel, D. G., Amadei, C. A., Campbell, J. R., Brault, J.-M., Zierler, A., & Veillard, J. (2022). *Strengthening public health surveillance through wastewater testing: An essential investment for the COVID-19 pandemic*. World Bank. https://openknowledge.worldbank.org/handle/10986/36852

Medema, G., Heijnen, L., Elsinga, G., Italiaander, R., & Brouwer, A. (2020). Presence of SARS-CoV-2 RNA in sewage and correlation with reported COVID-19 prevalence in the early stage of the epidemic in the Netherlands. *Environmental Science & Technology Letters*, *7*(7), 511–516. https://doi.org/10.1021/acs.estlett.0c00357

Ministry of the Environment, Conservation and Parks. (2022, September 16). *COVID‑19 wastewater monitoring*. Retrieved February 12, 2023, from https://www.ontario.ca/page/covid-19-wastewater-

monitoring

Mondal, S., Feirer, N., Brockman, M., Preston, M. A., Teter, S. J., Ma, D., Goueli, S. A., Moorji, S., Saul, B., & Cali, J. J. (2021). A direct capture method for purification and detection of viral nucleic acid enables epidemiological surveillance of SARS-CoV-2. *Science of the Total Environment*, *795*, 148834. https://doi.org/10.1016/j.scitotenv.2021.148834

Paul, D., Kolar, P., & Hall, S. G. (2021). A review of the impact of environmental factors on the fate and transport of coronaviruses in aqueous environments. *npj Clean Water*, *4*(1). https://doi.org/10.1038/s41545-020-00096-w

Pecson, B. M., Darby, E., Haas, C. N., Amha, Y. M., Bartolo, M., Danielson, R., Dearborn, Y., Di Giovanni, G., Ferguson, C., Fevig, S., Gaddis, E., Gray, D., Lukasik, G., Mull, B., Olivas, L., Olivieri, A., Qu, Y., & SARS-CoV-2 Interlaboratory Consortium. (2021). Reproducibility and sensitivity of 36 methods to quantify the SARS-CoV-2 genetic signal in raw wastewater: Findings from an interlaboratory methods evaluation in the U.S. *Environmental Science: Water Research & Technology*, *7*(3), 504–520. https://doi.org/10.1039/D0EW00946F

Poison, A. (1977). A theory for the displacement of proteins and viruses with polyethylene glycol. *Preparative Biochemistry*, *7*(2), 129–154. https://doi.org/10.1080/00327487708061631

Public Health Ontario. (2022). *Epidemiologic summary: SARS-CoV-2 whole genome sequencing in Ontario, March 1, 2022* (p. 4). Queen's Printer for Ontario. https://www.publichealthontario.ca/-/media/documents/ncov/epi/covid-19-sars-cov2-whole-genome-sequencing-epi-summary.pdf

R Core Team. (2021). *R: A Language and Environment for Statistical Computing*. https://www.r-project.org/

Raaben, M., Einerhand, A. W. C., Taminiau, L. J. A., Van Houdt, M., Bouma, J., Raatgeep, R. H., Büller, H. A., De Haan, C. A. M., & Rossen, J. W. A. (2007). Cyclooxygenase activity is important for efficient replication of mouse hepatitis virus at an early stage of infection. *Virology Journal*, *4*, 1–5.

https://doi.org/10.1186/1743-422X-4-55

Rahimi, N. R., Fouladi-Fard, R., Aali, R., Shahryari, A., Rezaali, M., Ghafouri, Y., Ghalhari, M. R., Asadi-Ghalhari, M., Farzinnia, B., Conti Gea, O., & Fiore, M. (2021). Bidirectional association between COVID-19 and the environment: A systematic review. *Environmental Research*, *194*, 110692. https://doi.org/10.1016/j.envres.2020.110692

Respiratory Virus Infections Working Group. (2020). Canadian Public Health Laboratory Network: Prioritized support for northern, remote and isolated communities in Canada. *Canada Communicable Disease Report*, *46*(10), 322–323. https://doi.org/10.1.745/ccdr.v46i10a02

Robinson, C. A., Hsieh, H. Y., Hsu, S. Y., Wang, Y., Salcedo, B. T., Belenchia, A., Klutts, J., Zemmer, S., Reynolds, M., Semkiw, E., Foley, T., Wan, X. F., Winberg, C. G., Wenzel, J., Lin, C. H., & Johnson, M. C. (2022). Defining biological and biophysical properties of SARS-CoV-2 genetic material in wastewater. *Science of the Total Environment*, *807*, 150786. https://doi.org/10.1016/j.scitotenv.2021.150786

Safford, H. R., Shapiro, K., & Bischel, H. N. (2022). Opinion: Wastewater analysis can be a powerful public health tool—If it's done sensibly. *Proceedings of the National Academy of Sciences*, *119*(6), e2119600119. https://doi.org/10.1073/pnas.2119600119

Schoeman, D., & Fielding, B. C. (2019). Coronavirus envelope protein: Current knowledge. *Virology Journal*, *16*(1), 69. https://doi.org/10.1186/s12985-019-1182-0

Simpson, A., Topol, A., White, B. J., Wolfe, M. K., Wigginton, K. R., & Boehm, A. B. (2021). Effect of storage conditions on SARS- CoV-2 RNA quantification in wastewater solids. *PeerJ*, *9*, e11933. https://doi.org/10.7717/peerj.11933

Sinclair, R. G., Rose, J. B., Hashsham, S. A., Gerba, C. P., & Haase, C. N. (2012). Criteria for selection of surrogates used to study the fate and control of pathogens in the environment. *Applied and Environmental Microbiology*, *78*(6), 1969–1977. https://doi.org/10.1128/AEM.06582-11

Swango, K. L., Timken, M. D., Chong, M. D., & Buoncristiani, M. R. (2006). A quantitative PCR assay

for the assessment of DNA degradation in forensic samples. *Forensic Science International*, *158*(1),

14–26. https://doi.org/10.1016/j.forsciint.2005.04.034

Torii, S., Furumai, H., & Katayama, H. (2021). Applicability of polyethylene glycol precipitation

followed by acid guanidinium thiocyanate-phenol-chloroform extraction for the detection of SARS-

CoV-2 RNA from municipal wastewater. *Science of The Total Environment*, *756*, 143067.

https://doi.org/10.1016/j.scitotenv.2020.143067

Vijgen, L., Keyaerts, E., Moës, E., Maes, P., Duson, G., & Van Ranst, M. (2005). Development of one-

step, real-time, quantitative reverse transcriptase PCR assays for absolute quantitation of human

coronaviruses OC43 and 229E. *Journal of Clinical Microbiology*, *43*(11), 5452–5456.

https://doi.org/10.1128/JCM.43.11.5452-5456.2005

Wellings, F. M., Lewis, A. L., & Mountain, C. W. (1976). Demonstration of solids associated virus in

wastewater and sludge. *Applied and Environmental Microbiology*, *31*(3), 354–358.

https://doi.org/10.1128/aem.31.3.354-358.1976

World Health Organization. (2022). *Environmental surveillance for SARS-CoV-2 to complement public*

health surveillance: Interim guidance, 14 April 2022. World Health Organization.

https://apps.who.int/iris/handle/10665/353158

Wu, F., Zhang, J., Xiao, A., Gu, X., Lee, L., Armas, F., & Kauffman, K. (2020). SARS-CoV-2 titers in

wastewater are higher than expected from clinically confirmed cases. *mSystems*, *5*(4), 1–9.

https://doi.org/10.1128/mSystems.00614-20

Wurtzer, S., Waldman, P., Ferrier-Rembert, A., Frenois-Veyrat, G., Mouchel, J. M., Boni, M., Maday, Y.,

Marechal, V., & Moulin, L. (2021). Several forms of SARS-CoV-2 RNA can be detected in

wastewaters: Implication for wastewater-based epidemiology and risk assessment. *Water Research*,

198, 117183. https://doi.org/10.1016/j.watres.2021.117183

Wurtzer, S., Waldman, P., Levert, M., Cluzel, N., Almayrac, J. L., Charpentier, C., Masnada, S., Gillon-
Ritz, M., Mouchel, J. M., Maday, Y., Boni, M., Moulin, L., Marechal, V., Le Guyader, S., Bertrand,
I., Gantzer, C., Descamps, D., Charpentier, C., Houhou, N., … Pawlotsky, J. M. (2022). SARS-
CoV-2 genome quantification in wastewaters at regional and city scale allows precise monitoring of
the whole outbreaks dynamics and variants spreading in the population. *Science of the Total
Environment*, *810*, 152213. https://doi.org/10.1016/j.scitotenv.2021.152213

Ye, Y., Ellenberg, R. M., Graham, K. E., & Wigginton, K. R. (2016). Survivability, partitioning, and
recovery of enveloped viruses in untreated municipal wastewater. *Environmental Science &
Technology*, *50*(10), 5077–5085. https://doi.org/10.1021/acs.est.6b00876

Zhang, T., Breitbart, M., Lee, W. H., Run, J. Q., Wei, C. L., Soh, S. W. L., Hibberd, M. L., Liu, E. T.,
Rohwer, F., & Ruan, Y. (2006). RNA viral community in human feces: Prevalence of plant
pathogenic viruses. *PLoS Biology*, *4*(1), 0108–0118. https://doi.org/10.1371/journal.pbio.0040003

Figure 1

Figure 2

Figure 3

12,000 *g*, 1.5 h, no brake

4 mL → Amicon Ultra-4

15 mL → Amicon Ultra-15

40 mL → Centricon Plus-70
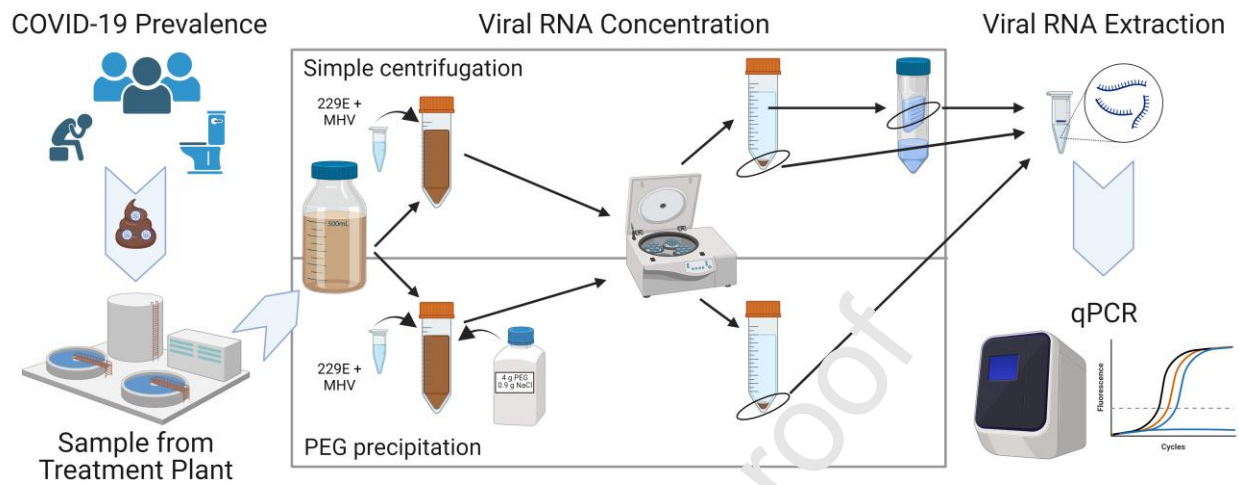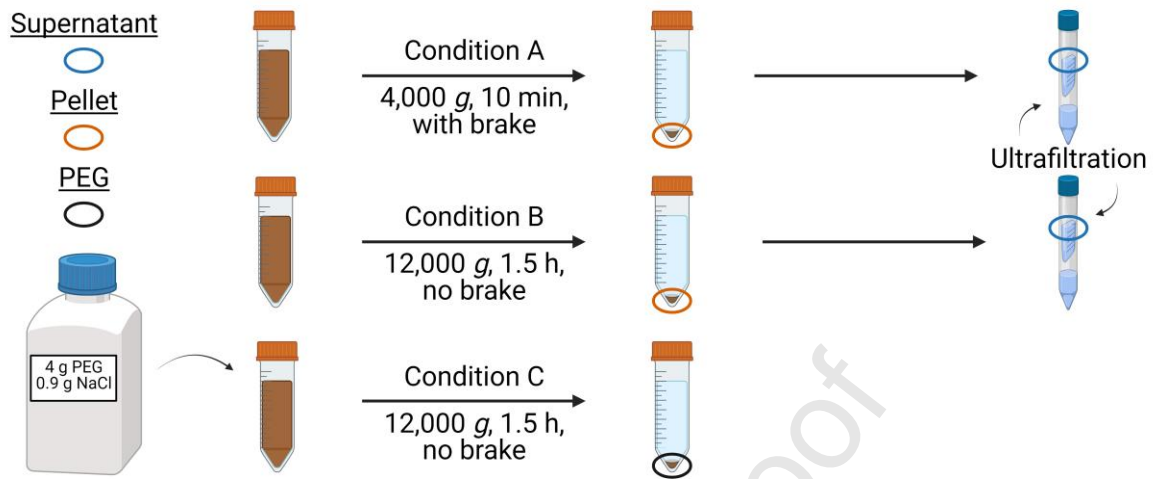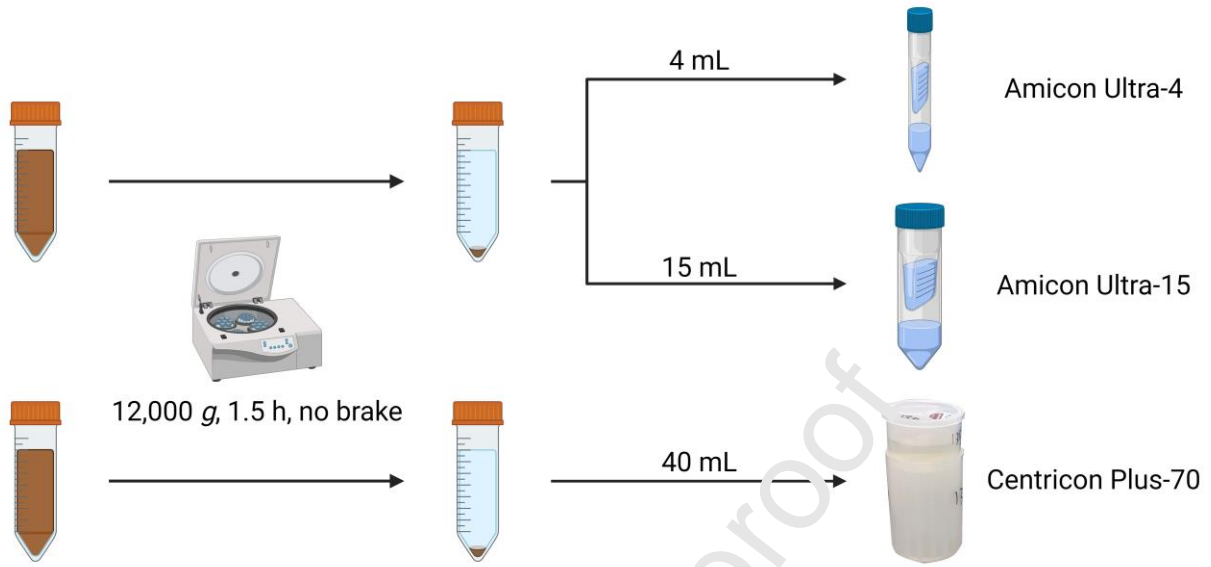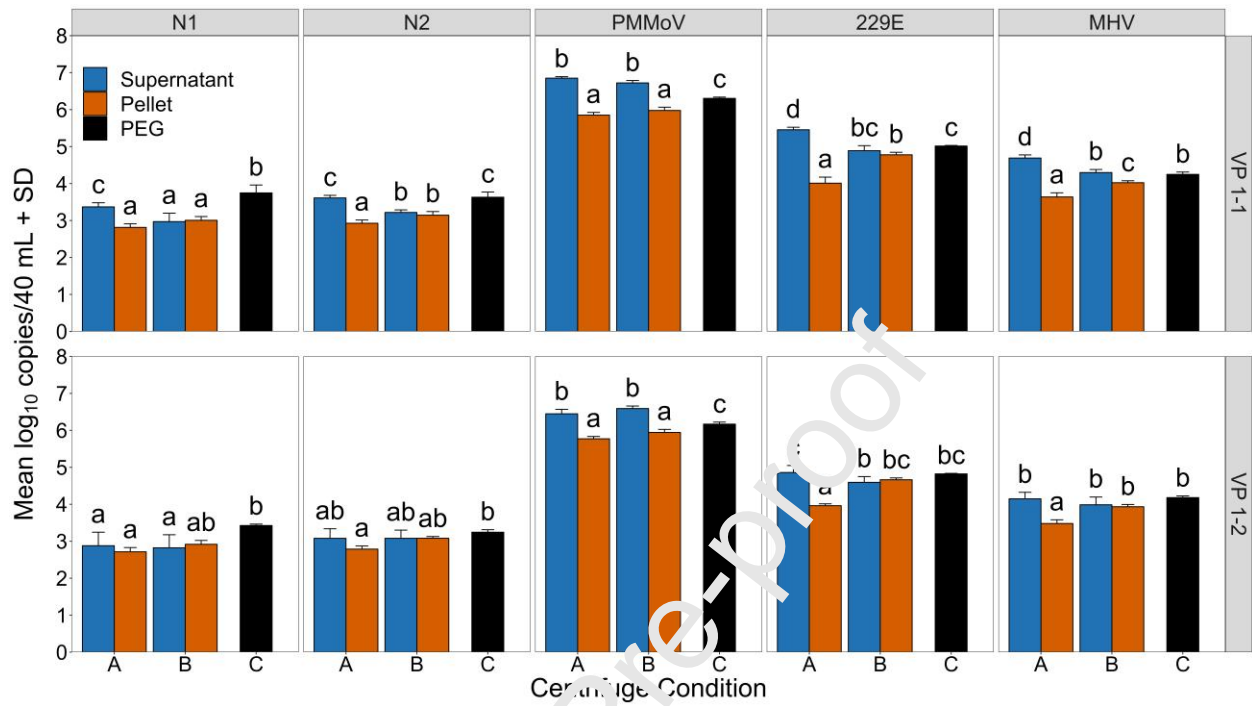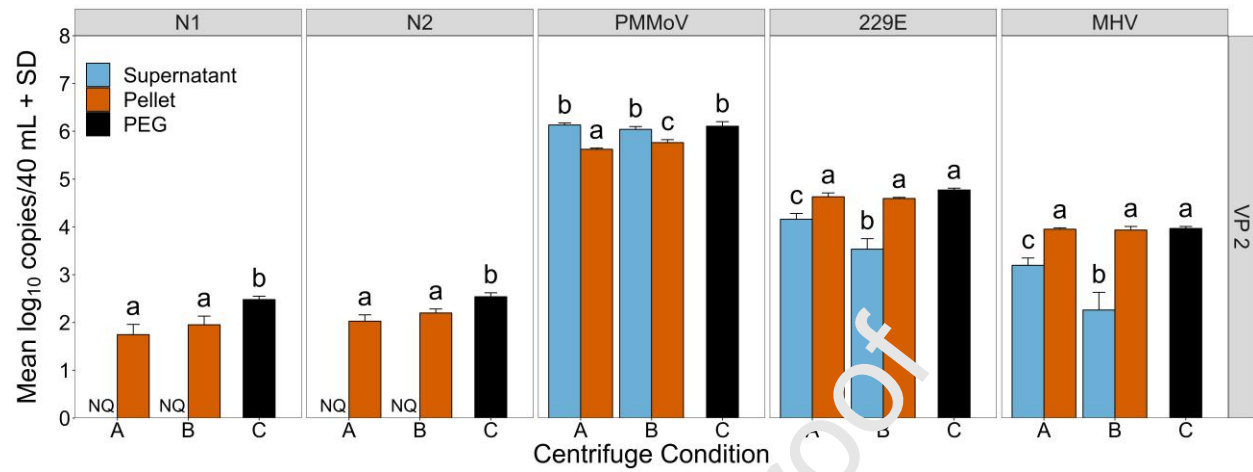
Figure 4
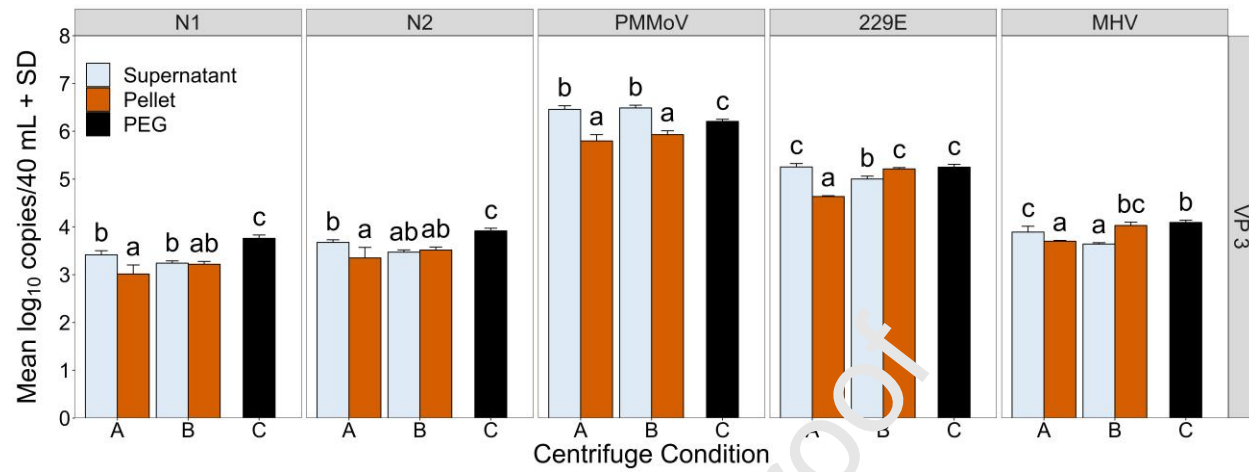
Figure 5

Figure 6

Figure 7
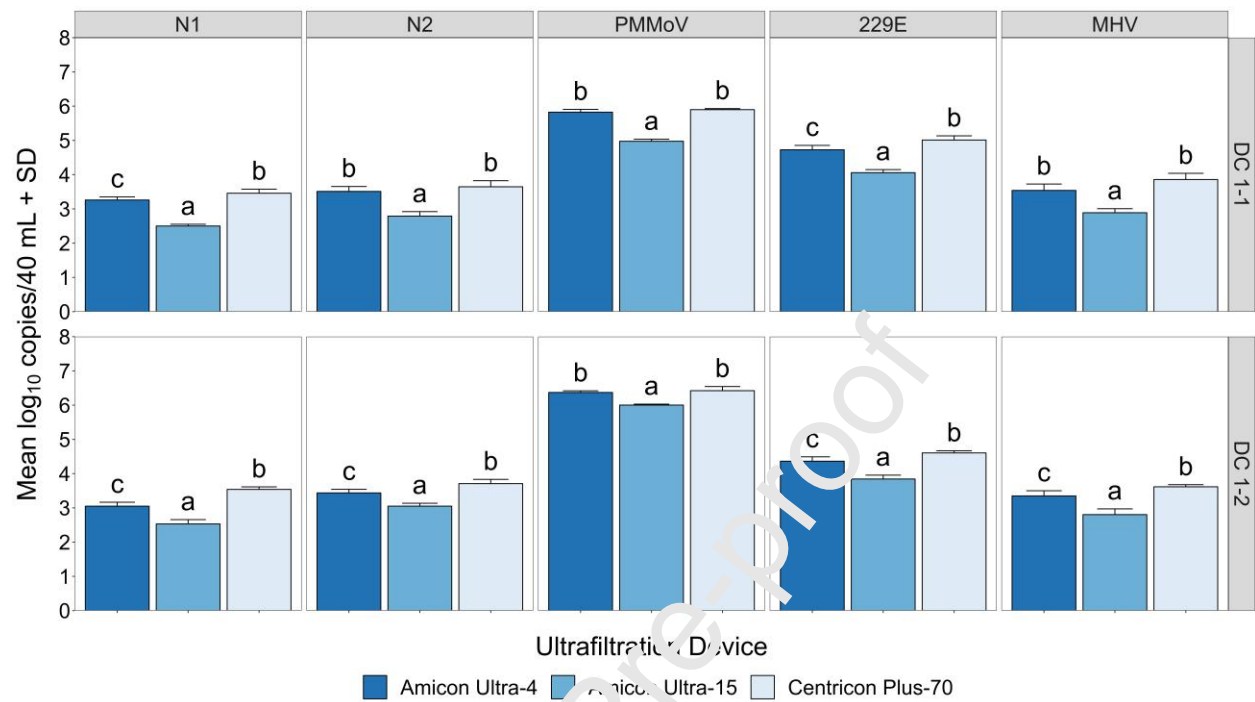
Table 1. Collection and extraction dates for the wastewater samples.

Experiment	Contributing Proportion[a]	Reported Case Count (Total of Previous 14 Days)[b]	Collection Date	Extraction Date	Dominant SARS-CoV-2 Strain[c]
VP 1-1	33% Clarkson	4359	Apr. 21, 2021	Apr. 22, 2021	Alpha
	67% GE Booth	8502			
VP 1-2	50% Clarkson	3352	May 7, 2021	May 10, 2021	Alpha
	50% GE Booth	6783			
VP 2	50% GE Booth	886	Sep. 21, 2021	Sep. 25, 2021	Delta
	25% Clarkson	396	Sep. 22, 2021		
	25% GE Booth	865	Sep. 22, 2021		
VP 3	10% Clarkson	5717	Jan. 19, 2022	Jan. 29, 2022	Omicron
	90% Clarkson	3058	Jan. 27, 2022		
DC 1-1	100% Kitchener	2597	Dec. 30, 2021	Jan. 8, 2022	Omicron
DC 1-2	100% Clarkson	5717	Jan. 19, 2022	Jan. 22, 2022	Omicron

Abbreviations: VP = viral partitioning; DC = ultrafiltration device comparison.

[a] Proportion of wastewater that was pooled for subsequent sample analysis.

[b] COVID-19 cases are by episode date as a rolling sum of the previous 14 days and are listed for each treatment plant based on the collection date. The data for the reported cases were extracted on December 14, 2022, from the Ontario Wastewater Surveillance Data and Visualization Hub which was developed by the Ministry of the Environment, Conservation and Parks (MECP) under the WSI (MECP 2022).

[c] Dominant SARS-CoV-2 strain during the collection period was based on proportion throughout Ontario, Canada (Public Health Ontario, 2022).

CRediT author statement

Patrick R. Breadner: Conceptualization, Methodology, Validation, Formal analysis, Investigation, Writing - Original Draft, Writing - Review & Editing, Visualization

Hadi A. Dhiyebi: Conceptualization, Methodology, Validation

Azar Fattahi: Writing - Review & Editing

Nivetha Srikanthan: Conceptualization, Methodology, Project administration

Samina Hayat: Methodology

Marc G. Aucoin: Resources

Scott J. Boegel: Resources

Leslie M. Bragg: Resources, Writing - Review & Editing

Paul M. Craig: Methodology, Validation

Yuwei Xie: Conceptualization

John P. Giesy: Funding acquisition, Writing - Review & Editing

Mark R. Servos: Conceptualization, Methodology, Validation, Supervision, Writing - Review & Editing, Funding acquisition

Declaration of interests

☒The authors declare that they have no known competing financial interests or personal relationships that could have appeared to influence the work reported in this paper.

☐The authors declare the following financial interests/personal relationships which may be considered as potential competing interests:

Graphical abstract
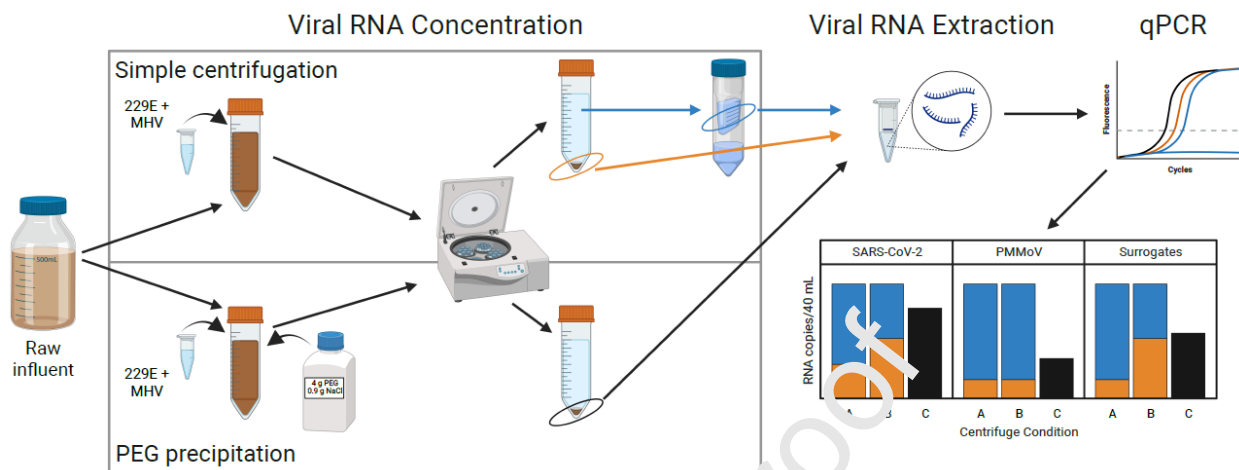
Highlights

- Partitioning of SARS-CoV-2 and PMMoV in wastewater differ and are context dependent

- A large proportion of viral RNA remains in the supernatant after centrifugation

- Use of different ultrafiltration devices can affect interpretation of partitioning

- Under some conditions, MHV and 229E surrogates partition similarly to SARS-CoV-2

Graphics Abstract

COVID-19 Prevalence
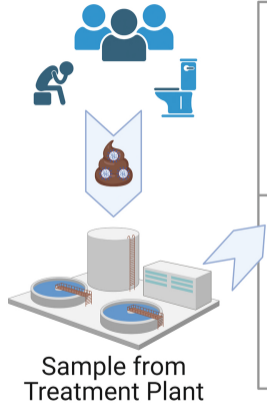
Viral RNA Concentration
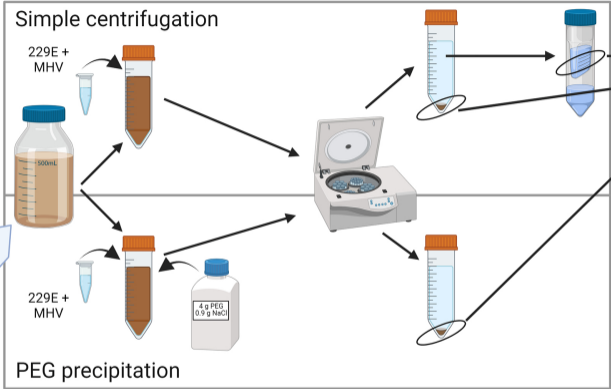
Simple centrifugation

229E + MHV

500mL

Sample from Treatment Plant

229E + MHV

4 g PEG 0.9 g NaCl

PEG precipitation

Viral RNA Extraction
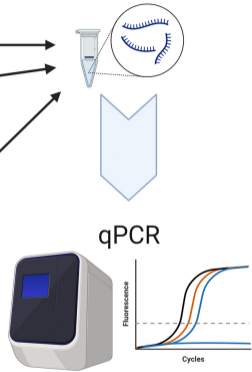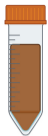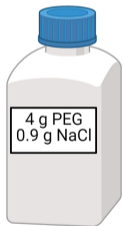
qPCR

Fluorescence

Cycles

Figure 1

Figure 2

4 mL — Amicon Ultra-4

15 mL — Amicon Ultra-15
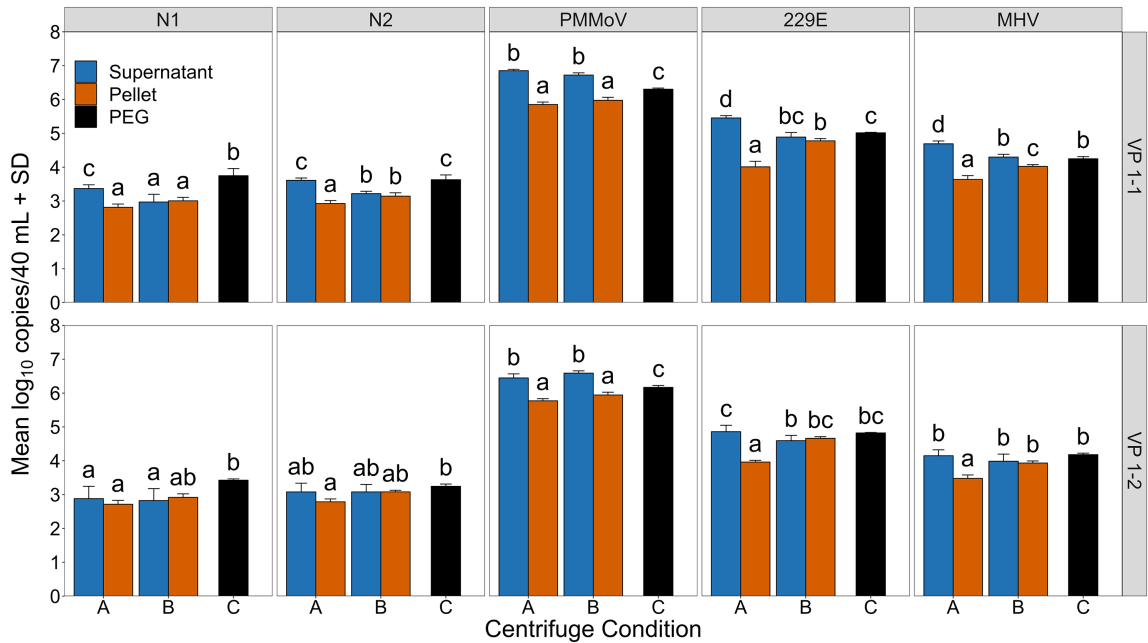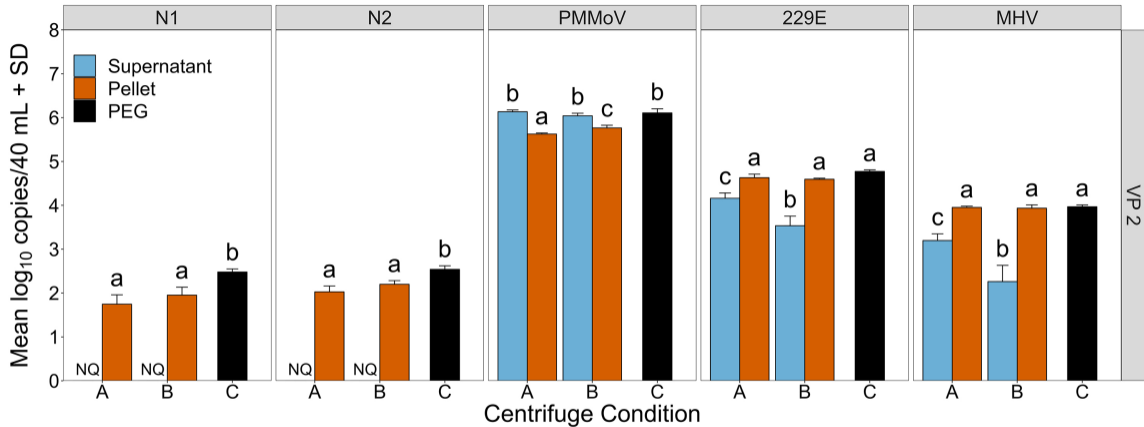
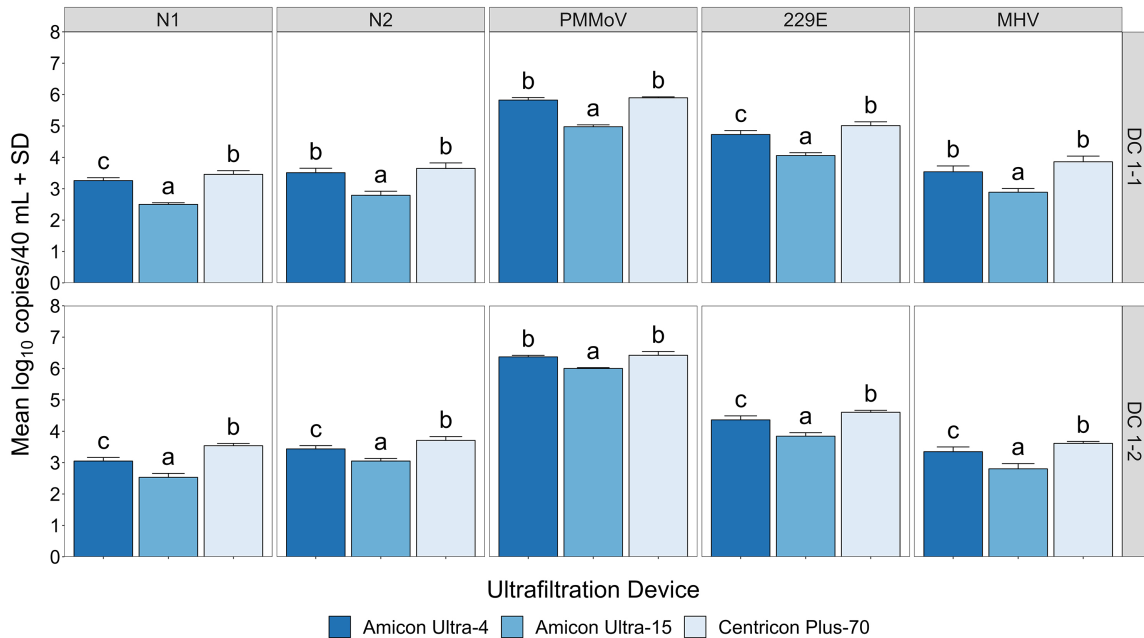12,000 g, 1.5 h, no brake

40 mL — Centricon Plus-70
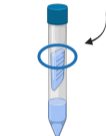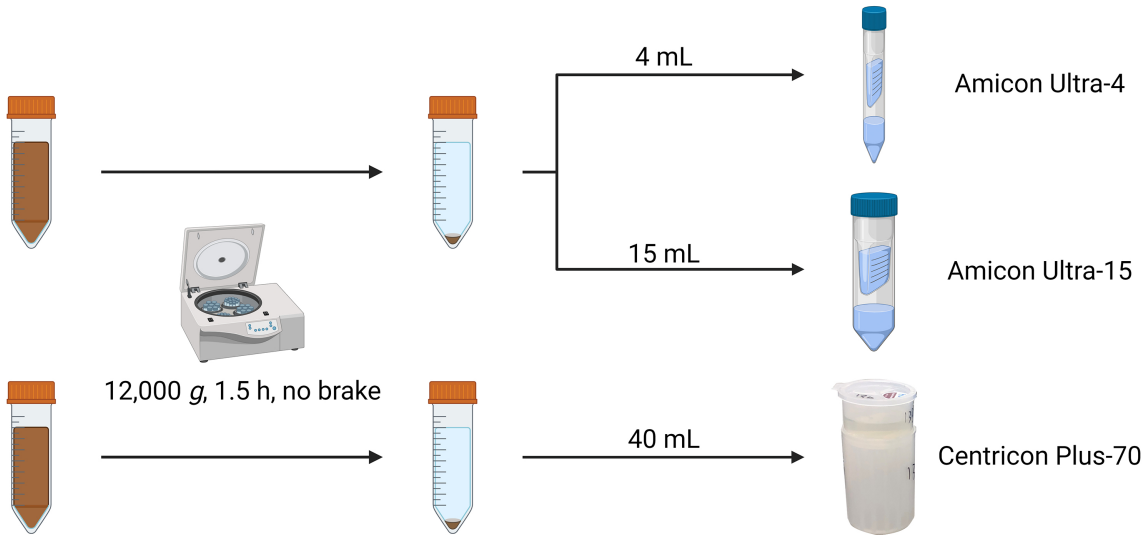
Figure 3

Figure 4

Figure 5

Figure 6

Figure 7